Human Molecular Genetics, 2014, Vol. 23, No. 23 **6286–6301**
doi:10.1093/hmg/ddu348
Advance Access published on July 2, 2014

Early miR-155 upregulation contributes to neuroinflammation in Alzheimer's disease triple transgenic mouse model

Joana R. Guedes[1,2,5], Carlos M. Custódia[3], Ricardo J. Silva[3], Luís P. de Almeida[4,5], Maria C. Pedroso de Lima[3,5] and Ana L. Cardoso[5,*]

[1]Doctoral Programme in Experimental Biology and Biomedicine, CNC – Center for Neuroscience and Cell Biology, University of Coimbra, 3004-517 Coimbra, Portugal, [2]Institute for Interdisciplinary Research, University of Coimbra, 3030-789 Coimbra, Portugal, [3]Department of Life Sciences, Faculty of Science and Technology, University of Coimbra, 3001-401, Coimbra, Portugal, [4]Laboratory of Pharmaceutical Technology, Faculty of Pharmacy, University of Coimbra, 3000-548 Coimbra, Portugal and [5]CNC – Center for Neuroscience and Cell Biology, University of Coimbra, 3004-517 Coimbra, Portugal

Received April 16, 2014; Revised and Accepted June 30, 2014

MicroRNAs (miRNAs) have emerged as a class of small, endogenous, regulatory RNAs that exhibit the ability to epigenetically modulate the translation of mRNAs into proteins. This feature enables them to control cell phenotypes and, consequently, modify cell function in a disease context. The role of inflammatory miRNAs in Alzheimer's disease (AD) and their ability to modulate glia responses are now beginning to be explored. In this study, we propose to disclose the functional role of miR-155, one of the most well studied immune-related miRNAs in AD-associated neuroinflammatory events, employing the 3xTg AD animal model. A strong upregulation of miR-155 levels was observed in the brain of 12-month-old 3xTg AD animals. This event occurred simultaneously with an increase of microglia and astrocyte activation, and before the appearance of extracellular Aβ aggregates, suggesting that less complex Aβ species, such as Aβ oligomers may contribute to early neuroinflammation. In addition, we investigated the contribution of miR-155 and the c-Jun transcription factor to the molecular mechanisms that underlie Aβ-mediated activation of glial cells. Our results suggest early miR-155 and c-Jun upregulation in the 3xTg AD mice, as well as in Aβ-activated microglia and astrocytes, thus contributing to the production of inflammatory mediators such as IL-6 and IFN-β. This effect is associated with a miR-155-dependent decrease of suppressor of cytokine signaling 1. Furthermore, since c-Jun silencing decreases the levels of miR-155 in Aβ-activated microglia and astrocytes, we propose that miR-155 targeting can constitute an interesting and promising approach to control neuroinflammation in AD.

INTRODUCTION

Alzheimer's disease (AD), the most common form of elderly dementia, is characterized at the cellular and molecular level by pathological hallmarks that include the presence of extracellular senile plaques, intraneuronal phosporylated-τ aggregates, neuronal death and both local and systemic inflammation. The most important non-cellular component of senile plaques is β-amyloid (Aβ), a peptide resulting from the tandem cleavage of the amyloid precursor protein (APP) by β-secretase and γ-secretase. This peptide is able to self-aggregate originating Aβ dimers, Aβ oligomers and, at a more complex stage, Aβ fibrils. The cellular components of Aβ plaques include dystrophic neuritis, cell debris and activated microglia and astrocytes (1).

In the last decade, the neuroinflammatory component of AD has been subject of intense debate. The chronic deposition of Aβ in the brain stimulates the persistent activation of astrocytes and microglia cells, leading to cell proliferation and overproduction of inflammatory mediators, such as cytokines, chemokines and nitric oxide (NO), which are responsible for the attraction of more astrocytes and microglia cells to the sites of Aβ deposition (2–4), as well as for the migration of peripheral mononuclear phagocytes to the brain (5). Despite the intense investigation in this field, the nature of astrocytes and microglia interaction

*To whom correspondence should be addressed at: Center for Neuroscience and Cell Biology, University of Coimbra, Largo Marquês de Pombal, 3004-517 Coimbra, Portugal. Tel: +351 239820190; Fax: +351 239826798; Email: alcardoso@ci.uc.pt

with Aβ remains controversial with respect to the strength of cell response to different Aβ forms and their neurotoxic or neuroprotective role in AD. On one hand, the excessive production of proinflammatory mediators promotes chronic neuronal toxicity but, on the other hand, microglia and astrocytes have been shown to help clear Aβ deposits, delaying disease progression (6,7). Nevertheless, all studies performed so far strongly suggest an important involvement of inflammatory pathways in the pathophysiology of AD (8,9) and reinforce the need to explore inflammation-related genes in therapeutics and diagnosis.

Although it is well documented that microglia constitutes the cellular type responsible for initiating the innate immune response against Aβ in the brain, it is becoming increasingly clear that astrocytes also play a critical role in the amplification of inflammatory and neurotoxic processes. The interaction between astrocytes and microglia cells has been studied in a physiological and pathological context, demonstrating that astrocytes are activated by microglia-released factors (10,11) and also by Aβ (12), these serving as immunomodulators of microglia-related immune responses. In glial cells, Aβ is recognized through Toll-like receptors (TLRs) 4 and 6 in the presence of CD36 (13–15). The activation of TLR4 leads to: early nuclear factor-κB (NF-κB) activation and tumor necrosis factor (TNF-α) production; delayed Janus tyrosine kinase 1/signal transducer and activator of transcription factors 1 (Jak1/Stat1) activation, which is regulated by Jun N-terminal kinase (JNK), resulting in the expression of the suppressor of cytokine signaling 1 (SOCS-1), which negatively regulates cytokines; and activation of the signaling pathway involving the mitogen-activated protein kinases (16). These intracellular signaling pathways are also associated with activation of the activator protein-1 (AP-1) transcription factor (which is composed of a dimer of c-Jun and c-Fos) by JNK that is related with apoptosis and inflammation. Neuronal apoptosis can be triggered by Aβ through activation of JNK (17) and, in glial cells, the inhibition of JNK activation leads to the production of interleukin 10, an anti-inflammatory cytokine (18). Interestingly, c-Jun was found to be activated in AD brains (19) and our previous data have shown that silencing of c-Jun resulted not only in a blockade of neuronal death, but also in a decrease of brain inflammation in an excitotoxic lesion model *in vivo* (20). These results suggest a clear involvement of c-Jun in apoptosis and inflammatory responses in AD.

Small endogenous non-coding RNAs, also known as microRNAs (miRNAs) regulate gene expression primarily at the post-transcriptional level, exerting their function by targeting complementary mRNA molecules and inhibiting their translation through binding to the 3′UTR. Their involvement in almost all biological functions and their capacity to promote the fine regulation of intracellular processes by targeting multiple mRNAs simultaneously make them a class of emerging molecules with potential to be used in therapy and diagnostics. Several miRNA networks, including miRNAs related with innate immunity and neuroinflammation have been found to be deregulated in AD (21–23). MiR-155 is considered a pro-inflammatory miRNA and has been shown to play a central role in the regulation of the innate immune response, through modulation of cytokine and chemokine production (24–26). In 2007, O'Connel *et al.* (27) first described miR-155 as a key player in macrophage inflammatory response following TLR activation and suggested that its upregulation was dependent on the JNK pathway. Moreover, in 2013, Onyeagucha *et al.* (28) suggested that miR-155 expression is regulated by the AP-1 transcription factor. In fact, these authors observed that attenuation of AP-1 activation through pharmacological inhibition of MEK activation or genetic inhibition of c-Jun activation, using dominant negative c-Jun (TAM67), suppressed miR-155 induction. Interestingly, our laboratory showed that miR-155 also increases in microglia, following lipopolysaccharide (LPS) stimulation (25), and regulates SOCS-1 levels, as well as cytokine and NO production, thus providing evidence that this miRNA can exert a pro-inflammatory role both in the peripheral immune system and the brain. Moreover, some observations suggest that miR-155 also plays a role in gene regulatory networks in astrocytes, due to its increased expression upon astrocyte activation (29), and is involved in proinflammatory cytokine upregulation in these cells by targeting SOCS-1 mRNA (30).

Given the importance of miR-155 and c-Jun in inflammatory responses, in this work we proposed to investigate the role of these two cell modulators in Aβ-mediated neuroinflammation in the context of AD.

RESULTS

Inflammation precedes senile plaque deposition in the 3xTg AD model

Studies showing the co-localization of activated microglia and astrocytes with Aβ plaques in the post-mortem AD brain suggest the involvement of inflammatory pathways in disease progression (31). However, these evidences do not clarify the role of the immune system in the early stages of AD. The lack of human brain samples at early stages that could provide information on the inflammatory molecular mechanisms that precede the deposition of Aβ plaques led us to study the involvement of these signaling pathways in the 3xTg mice model of AD. Although human studies have been essential to establish inflammation as an AD hallmark, experiments using transgenic AD mice allow associations between chronic inflammation and cognitive deficits, as well as the opportunity to test *in vivo* inflammation-based therapeutic strategies. The 3xTg mouse model of AD, developed in LaFerla's laboratory, progressively develops Aβ and τ pathology, with a temporal- and regional-specific profile that closely mimics its development in the human AD brain (32). According to Janelsins *et al.* (33), this mouse model also presents brain inflammation at early stages of the disease, as revealed by the increase in the number of $F4/80^{+}$ microglia/macrophages. At 6 months, 3xTg AD mice already displayed elevated levels of intraneuronal Aβ, hyperphosporylated-τ and microglia activation. However, only at 12 months it was possible to observe an increase of TFN-α receptor II-related mRNAs, which correlated with neuronal death (34).

Based on the above findings, our studies were performed in both 3- and 12-month-old (3 and 12 months) 3xTg AD mice. These time points allowed studying the involvement of microglia and astrocytes, two different cell types implicated in neuroinflammation, at different stages of disease progression. Moreover, since studies in humans and mice have established an early inflammatory component in AD, we aimed to disclose the contribution of miR-155 to this process. In order to correlate temporarily the appearance of Aβ plaques and neuroinflammation hallmarks,

such as microglia activation, astrocyte proliferation and production of inflammatory cytokines, we performed immunohistochemistry studies in coronal brain sections of 3- and 12-months 3xTg AD animals, which were labeled both for microglia and astrocyte protein markers, ionized calcium-binding adapter molecule 1 (IBA-1) and glial fibrillary acidic protein (GFAP) (Fig. 1), respectively, and also for the Aβ peptide (Fig. 2). No significant changes were observed in 3xTg AD animals with respect to age-matched wild-type (WT) animals at 3 months (Supplementary Material, Fig. S1) in what concerns the number and phenotype of microglia and astrocytes. However, at 12 months, we observed extensive microglia and astrocyte proliferation in the hippocampus and cortex of 3xTg AD mice. These two brain regions are known to be strongly involved in AD and suffer the first loss of neuronal circuits in this disease (35). As shown in Figure 1, microglia from both the prefrontal cortex (Fig. 1B) and hippocampus (Fig. 1C) of 3xTg AD mice acquired an ameboid phenotype, characteristic of the transition from a resting to an activated state. This change was not observed in age-matched WT mice (Fig. 1D–F). Moreover, the number of microglia cells was highly increased in 3xTg AD animals with respect to WT mice. The same was true for astrocytes (Fig. 1G–I), especially in the hippocampus region. Since the presence of these neuroinflammatory features was only observed at 12 months, we further investigated if they were a consequence of the formation of intracellular or extracellular Aβ deposits. As expected, since intracellular human Aβ overproduction is one of the first neuropathological events in AD, intraneuronal Aβ immunostaining, using the WO-2 anti-human Aβ peptide, was found to be significantly enhanced in the hippocampus and prefrontal cortex of

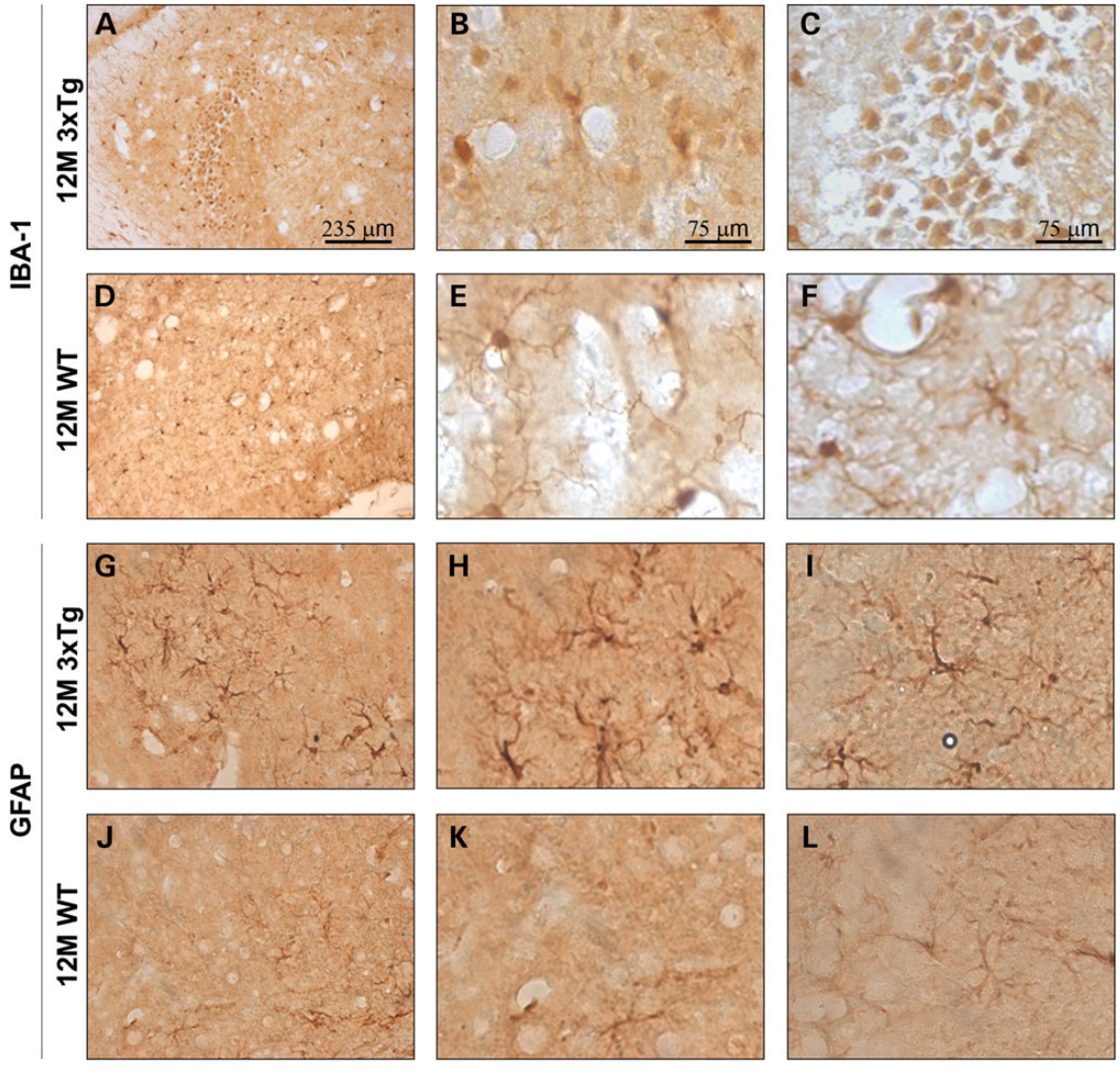

Figure 1. Microgliosis and astrogliosis in 3xTg AD animals. In order to identify astrocytes and microglia in the mouse brain, slices of 12-month 3xTg AD animals or their WT littermates were mounted in FluorSave™ Reagent on microscope slides and incubated with anti-IBA-1 or anti-GFAP antibodies to stain microglia and astrocytes, respectively. Following incubation with a biotinylated secondary antibody and visualization with 3,3′-diaminobenzidine tetrahydrochloride, pictures were taken under a Zeiss Axiovert microscope. Representative microscopy images of hippocampus (**A** and **D**) and cortex (**G** and **J**) are presented at ×200 magnification. A specific area of each image was zoomed 3× to obtain close-up images showing the ameboid (**B** and **C**) or ramified (**E** and **F**) morphology of microglia in each brain region. Astrocyte proliferation in the 3xTg AD animals (**H** and **I**) with respect to their WT littermates (**K** and **L**) can be observed at ×400 magnification for both brain regions. $n = 6$ animals for each experimental group.

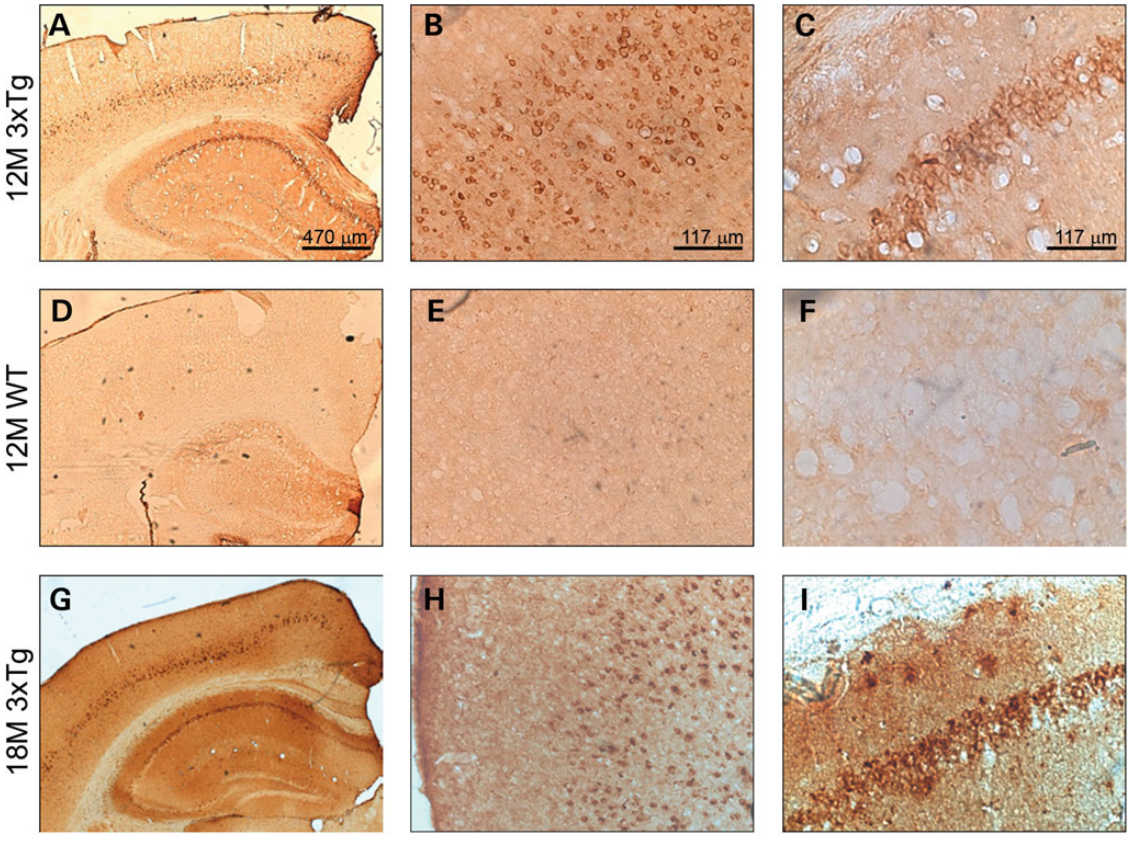

Figure 2. Intraneuronal and extracellular Aβ accumulation in 3xTg AD mice. In order to visualize Aβ deposition, brain slices of 3xTg AD animals and WT littermates were mounted in FluorSave™ Reagent on microscope slides and incubated with an anti-human Aβ peptide antibody to stain Aβ plaques. Following incubation with a biotinylated secondary antibody and visualization with 3,3′-diaminobenzidine tetrahydrochloride, pictures were taken under a Zeiss Axiovert microscope. Microscopy images of the hippocampus and cortex of 12-month 3xTg AD and WT animals and 18-month 3xTg AD animals (**A**, **D** and **G**) are presented at ×50 magnification and are representative of $n = 6$ animals for each experimental group. A specific area of each image was zoomed 4× to obtain close-up images of the cortex (**B**, **E** and **H**) and hippocampus (**C**, **F** and **I**). It is possible to observe the intracellular accumulation of Aβ in pyramidal CA1 and cortical neurons of 12-month 3xTg AD animals, but not in their WT aged-matched littermates. Extracellular senile plaques were only observed in 18-month 3xTg AD animals (I).

3xTg animals with both 3 (Supplementary Material, Fig. S1) and 12 months (Fig. 2A–C), whereas human Aβ positive cells were not detected in age-matched WT littermates (Fig. 2D–F), confirming the selectivity of the Aβ antibody and the presence of this hallmark of the disease. In this study, 12-month 3xTg AD mice did not present large extracellular deposits of Aβ in the cortex and hippocampus, as was observed in the hippocampus of 18-month 3xTg AD (Fig. 2G–I), where such deposits exhibited the characteristic round and diffuse Aβ brown stains. However, at 12 months, small immunoreactive dots could already be observed in the extracellular space. Therefore, our study suggests the existence of an early inflammatory response of both microglia cells and astrocytes in 3xTg AD mice, which precedes the formation of extracellular Aβ plaques but not intraneuronal Aβ accumulation or the presence of proto-fibrillary Aβ.

Taking into consideration the increase in the number of microglia cells and astrocytes observed in 3xTg AD mice, we investigated if the levels of molecular mediators of the immune response were also upregulated in these animals (Fig. 3). A significant increase in the mRNA levels of both interleukin-6 (IL-6) (Fig. 3A) and interferon beta (IFN-β) (Fig. 3B) was detected by qRT-PCR in 3xTg AD animals at 12 months, whereas no significant differences were found for TNF-α and IL-1β, between 3xTg AD animals and their WT littermates (data not shown). Since no extracellular Aβ plaques were visible in the 3xTg AD animals at 12 months, the age-dependent increase observed in IL-6 and IFN-β mRNA levels may be a response to the accumulation of intraneuronal Aβ or to the production of less complex extracellular Aβ species, such as Aβ dimers, oligomers and proto-fibrils that are not so easily detected by immunohistochemistry. Furthermore, at 3 months, the levels of both IL-6 and IFN-β were found to be downregulated in the 3xTg AD animals with respect to their WT littermates. These levels can be explained, in part, by our observation of miR-125b upregulation in 3-month 3xTg animals (Supplementary Material, Fig. S2). This miRNA is highly expressed in the brain and is considered an anti-inflammatory miRNA in macrophages (36), as well as a regulator of astrocyte proliferation (37). Interestingly, at 12 months, miR-125b expression is decreased in 3xTg AD animals compared with WT mice (Supplementary Material, Fig. S2), which correlates with astrogliosis and with the strong inflammatory phenotype found at this age.

MiR-155 is upregulated in the brain of the 3xTg AD model

As discussed before, miRNAs regulate gene expression at a post-transcriptional level and have been shown to be directly involved in the regulation of inflammatory pathways. MiRNAs have also

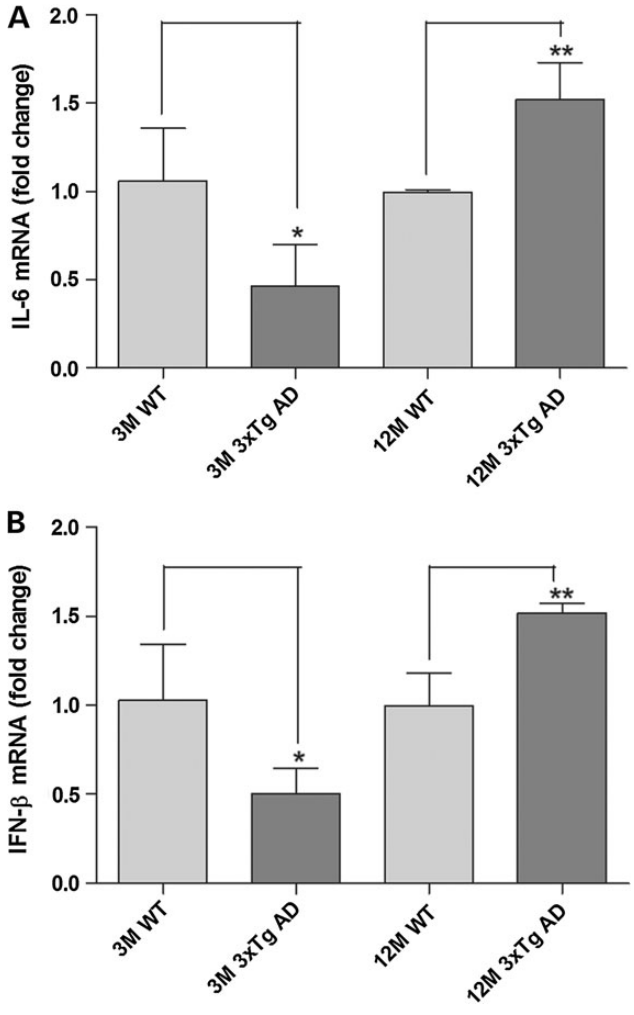

Figure 3. Cytokine production in 3xTg AD animals. Total RNA extracts containing hippocampal and cortical brain regions of 3xTg AD animals, at 3 and 12 months, or their WT littermates were used to quantify IL-6 (**A**) and IFN-β (**B**) mRNA levels by qRT-PCR. Results are expressed as mRNA fold change as compared with 3 or 12-month WT mice and are representative of $n = 6$ animals per experimental group. $^{*}P < 0.05$ and $^{**}P < 0.01$ with respect to age-matched WT littermates.

been directly related with neurodegeneration and global expression studies have revealed the deregulation of specific miRNAs in AD (38,39). These non-coding small RNA molecules are essential for neuronal survival and control of innate immune responses triggered by brain lesions or accumulation of aggregated proteins. MiR-155 is a proinflammatory miRNA, widely described in the peripheral immune system, which has been recently shown, by us and others, to be associated with neuroimmunity (25,40,41). Taking into consideration its important role in microglia (25) and astrocyte (40) function and our observation that both these cell types are activated in the 3xTg AD mouse model, we investigated the contribution of this miRNA to the Aβ-dependent inflammatory response in AD.

In order to analyze miR-155 expression in 3- and 12-month animals, total RNA was extracted from brain homogenates (brain without the olfactory bulb and cerebellum) and miR-155 levels were quantified by qRT-PCR. MiR-155 was found to be significantly upregulated in 3xTg AD mice at 12 months, these animals presented a 3-fold increase in miR-155 levels with respect to their WT littermates (Fig. 4A). In addition, we observed that 3-month 3xTg AD animals already exhibited increased expression of miR-155, albeit not statistically significant, and that the levels of this miRNA presented an age-dependent increase in 3xTg AD animals but not in WT animals. These results were consistent with *in situ* hybridization studies performed in coronal brain sections of 3- and 12-month 3xTg AD animals and WT littermates (Fig. 3B). In these experiments, a DIG-labelled (digoxigenin-labelled) locked nucleic acid (22) probe specific for the 5′ terminal of miR-155 was used to label miR-155. A specific U6 snRNA probe was used as positive control (data not shown). As expected, miR-155 labeling was strongly increased in brains slices of 12-month 3xTg AD mice when compared with 3-months transgenic animals and WT littermates. Nevertheless, 3-months 3xTg AD mice already presented a visible increase in miR-155 labeling in the hippocampus region, with respect to 3-month WT animals. Interestingly, the increase in miR-155 labeling was restricted almost exclusively to the cortex and hippocampus (Fig. 4B), the two regions where microglia and astrocyte activation had been previously observed.

In order to further investigate if astrocytes and microglia could be responsible for the observed upregulation of miR-155 in 3xTg AD animals, we measured the levels of this miRNA in *in vitro* cultures of both cell types upon exposure to Aβ. Since the contribution of different Aβ forms to neuroinflammation remains poorly understood, both N9 microglia and astrocyte primary cultures were incubated with two different species of the Aβ peptide, Aβ fibrils and Aβ oligomers. These Aβ species were prepared as described in the Materials and Methods, and the different aggregate sizes were confirmed using 4–16% Tris–Tricine SDS-PAGE gel electrophoresis. As can be observed in the Supplementary Material, Figure S8, the Aβ oligomers preparation did not present Aβ fibrils and only a small percentage of Aβ oligomers could be detected in the Aβ fibrils preparation (Supplementary Material, Table S1). The levels of miR-155 were quantified by qRT-PCR following a 24 h incubation period and LPS was used as a positive control in this experiment on the basis of our previous results showing that LPS is able to increase significantly miR-155 levels in both microglia (25) and astrocytes (unpublished data). We observed that miR-155 is upregulated upon incubation with Aβ fibrils in both microglia (Fig. 5A) and astrocytes (Fig. 5B). Regarding microglia, the exposure of N9 microglia cells to Aβ fibrils, at a concentration of 20 μM, triggered an overexpression of miR-155 similar to that obtained with LPS (8-fold). The same concentration of Aβ oligomers promoted a small increase in miR-155 levels, although this increase was not found to be statistically significant. In what concerns astrocytes, higher amounts of Aβ fibrils were necessary to promote a significant increase in miR-155. Thirty micromolar of Aβ fibrils promoted a 4-fold increase in miR-155 levels, while LPS induced a 10-fold increase. Once again, Aβ oligomers showed a tendency to promote miR-155 upregulation, but the results were not statistically significant. Importantly, no upregulation of miR-155 was detected in primary hippocampal neurons incubated with Aβ fibrils at the same concentrations (data not shown), confirming that the upregulation of miR-155 observed in 3xTg AD animals must originate in the phenotypic changes observed in microglia and astrocytes.

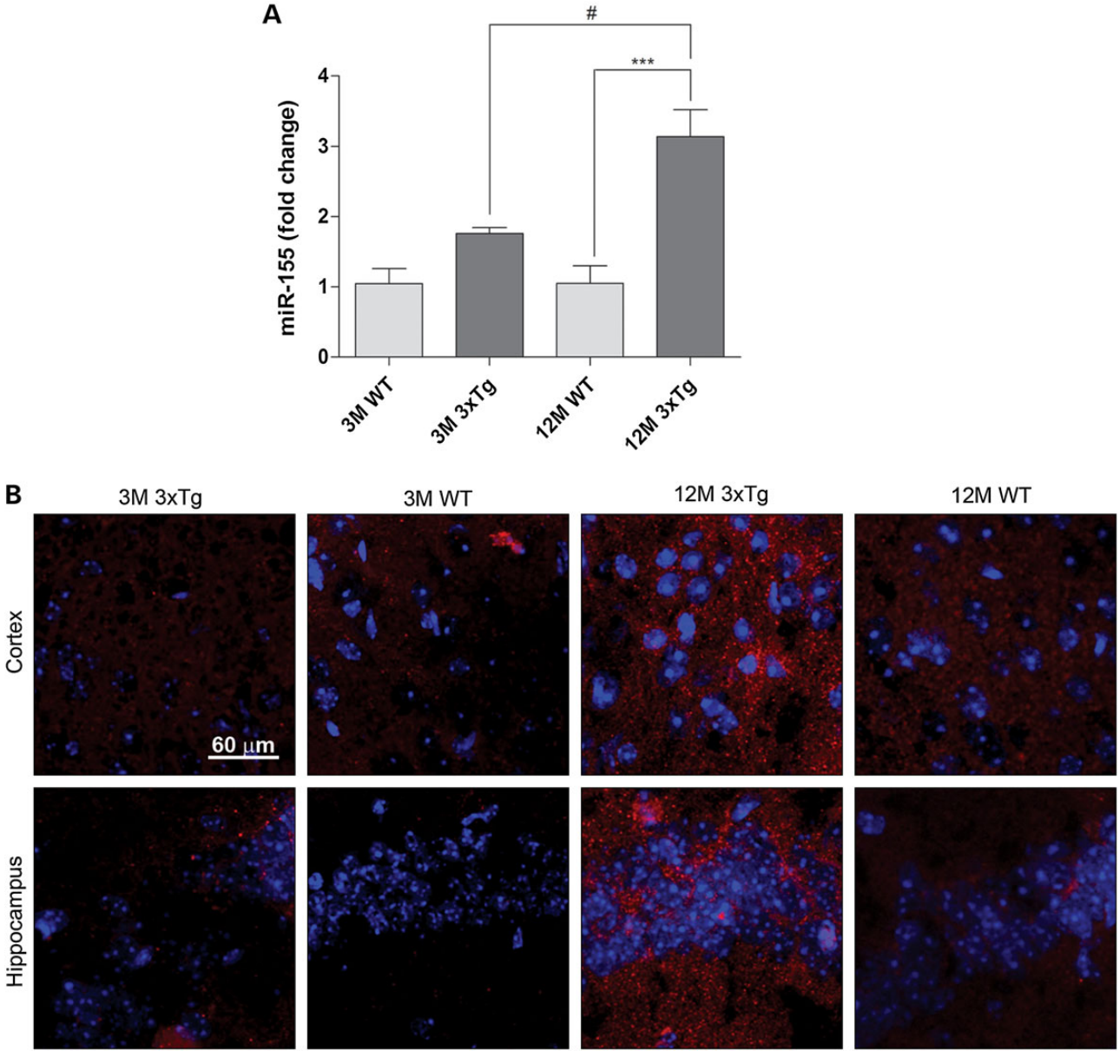

Figure 4. MiR-155 levels in 3xTg AD mice. Total RNA extracts containing hippocampal and cortical brain regions of 3xTg AD animals, at 3 and 12 months, or their age-matched WT littermates were used to quantify (**A**) miR-155 by qRT-PCR. Results are expressed as miRNA fold change with respect to 3-month WT mice. $^{***}P < 0.001$ with respect to age-matched WT littermates and $^{\#}P < 0.05$ with respect to 3-month 3xTg AD mice. (**B**) *In situ* hybridization was used to visualize miR-155 expression in brain slices of 3xTg AD animals and their WT littermates. The slices were labeled with a DIG-bound LNA probe specific for miR-155 detection (red), followed by nuclei labeling with Hoechst 33342 (blue) and mounted in microscope slides. Confocal images from the cortical and hippocampal regions of 3- and 12-months-old 3xTg AD animals and their WT littermates were acquired with a confocal Zeiss LSM 510 Meta microscope, using the ×60 oil objective. Both qRT-PCR and confocal results are representative of $n = 6$ animals per experimental group.

These results also suggest that Aβ fibrils are more efficient in promoting miR-155 expression *in vitro* than less complex Aβ species, such as oligomers.

Following our previous observation of an upregulation of IL-6 and IFN-β in 12-month 3xTg AD mice and, since it has been reported that miR-155 can influence cytokine production by interfering with the levels of several important immune modulators, such as SOCS-1, we measured the mRNA levels of these cytokines in N9 microglia cells and astrocyte primary cultures, following cell incubation with Aβ fibrils or oligomers (Fig. 5). As shown, both IL-6 and IFN-β were upregulated in Aβ-stressed microglia and astrocytes with respect to non-activated cells. N9 microglia cells presented an upregulation of IL-6, following a 24 h incubation period with Aβ fibrils or with the highest concentration of Aβ oligomers (Fig. 6A). However, the IL-6 expression peak occurs 30 min following N9 microglia cells exposure to Aβ fibrils, suggesting a fast inflammatory response to this stimulus, which is maintained during at least a 24 h period (Supplementary Material, Fig. S3A). IL-6 mRNA expression is slower and less prominent following microglia activation with

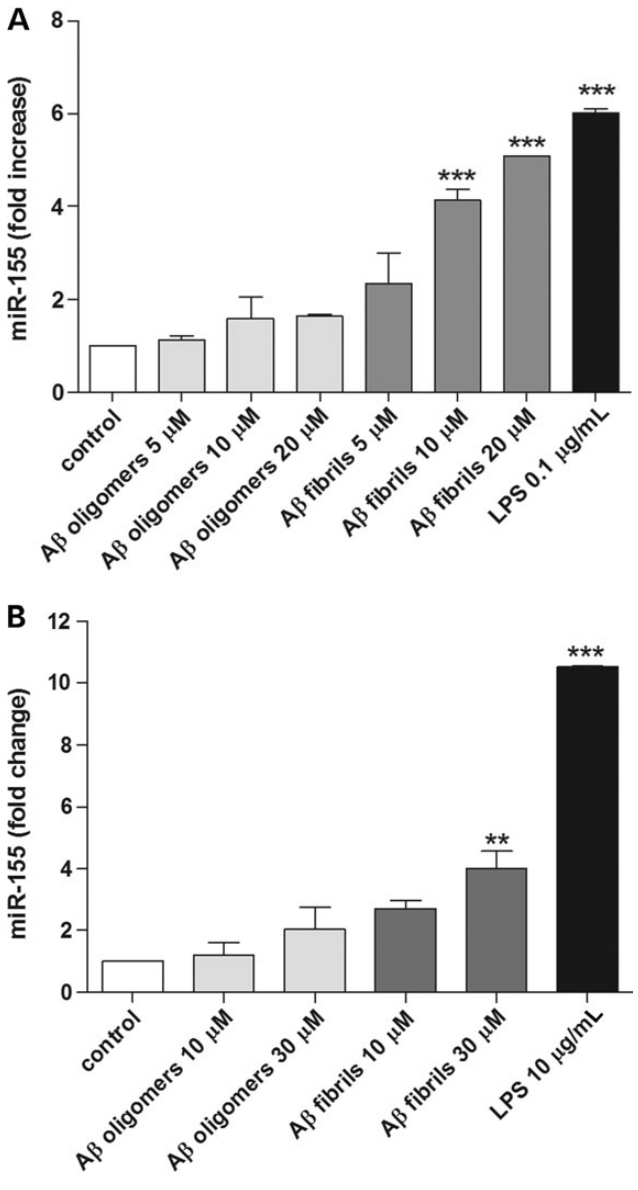

Figure 5. MiR-155 expression in Aβ-activated microglia and astrocyte cultures. N9 microglia cells or astrocyte primary cultures were plated and maintained in culture for 1 day before incubation with Aβ oligomers or Aβ fibrils. (**A**) N9 microglia cells were incubated with 5, 10 and 20 μM of Aβ for 24 h, while (**B**) astrocyte primary cultures were incubated with 10 and 30 μM of Aβ for the same period of time. Both cell types were incubated with LPS as a positive control (0.1 μg/ml in microglia and 10 μg/ml in astrocytes). Following the incubation period, total RNA was extracted from each condition and miR-155 levels were quantified by qRT-PCR. Results are expressed as miRNA fold change with respect to control (cells in the absence of stimulus) and are representative of three independent experiments performed in duplicate. $^{**}P < 0.01$ and $^{***}P < 0.001$with respect to control.

Aβ oligomers than with Aβ fibrils, showing only a 2-fold increase at 6 h and remaining constant until 24 h (Supplementary Material, Fig. S3A). Interestingly, and in contrast to IL-6, IFN-β was found to be more expressed in the presence of Aβ oligomers (Fig. 6C), presenting an expression peak at 18 h (Supplementary Material, Fig. S3C), although being also significantly increased in microglia cells stimulated with 20 μM of Aβ fibrils. The upregulation of IL-6 and IFN-β mRNAs in N9 microglia cells, in the presence of Aβ fibrils and Aβ oligomers, respectively, fully correlates with the secreted levels of both cytokines measured by ELISA (Supplementary Material, Fig. S4A and B). Furthermore, IL-4 and TNF-α release was also upregulated in N9 microglia incubated with Aβ fibrils, but not with Aβ oligomers (Supplementary Material, Fig. S4), suggesting that Aβ fibrils elicit a more robust inflammatory response. In what concerns astrocytes, only Aβ fibrils were able to upregulate IL-6 expression (Fig. 6B), with a 50-fold change with respect to non-activated cells, while IFN-β was only overexpressed upon cell incubation with 30 μM of Aβ oligomers (Fig. 6D). An interesting observation is that, although different Aβ forms lead to production of different levels of immune modulators in microglia and astrocytes, the pattern of the triggered immune responses is the same in both cell types. Indeed, while the pro-inflammatory cytokine IL-6 is upregulated in the presence of Aβ fibrils, the levels of the immunomodulatory cytokine IFN-β increase after exposure to Aβ oligomers.

Although we did not find differences in the levels of TNF-α and IL-1β in 3xTg AD mice, with respect to their WT littermates (data not shown), we were able to find a strong and early upregulation of both TNF-α and IL-1β in N9 microglia cells activated with Aβ fibrils or Aβ oligomers, at 2 h and 30 min, respectively (Supplementary Material, Fig. S3B and D). However, 24 h after Aβ exposure, we could only detect an increase in TNF-α secretion following incubation with Aβ fibrils (Supplementary Material, Fig. S4C). The observed increase in the mRNA levels of IL-1β and TNF-α did not translate in increased cytokine secretion for N9 cells exposed to Aβ oligomers. Moreover, the mRNA expression of both these cytokines was also found to be increased in astrocytes incubated with Aβ fibrils, but not in astrocytes exposed to Aβ oligomers (Supplementary Material, Fig. S5).

SOCS-1 is downregulated in the brain of the 3xTg AD model

The strong overexpression of miR-155 in the 3xTg AD mice led us to search for molecular targets of this miRNA involved in inflammatory signaling, whose downregulation could help explain the upregulation of IL-6 and IFN-β observed in the brain of 3xTg AD animals. As we and others have previously reported, SOCS-1 is a molecular target of miR-155 and its expression is decreased upon miR-155 upregulation (25,42). This protein is also considered to be an important protagonist in the regulation of the innate immune response. The activation of TLRs or cytokine receptors induces SOCS-1 expression, which acts in a negative feedback loop to allow the return of immune cells to basal conditions and avoid the overstimulation of the immune response (43). Moreover, SOCS-1 has already been proposed to play a role in CNS immunity and several studies have pointed its involvement in different neuropathological conditions (44).

Based on the above findings, we determined the levels of SOCS-1 in the 3xTg AD animals at 3 and 12 months and found that both mRNA and protein (Fig. 7) levels were dramatically decreased in 12-month 3xTg AD animals with respect to their WT littermates. As observed, the levels of SOCS-1 mRNA were already slightly decreased in 3-month 3xTg AD animals (Fig. 7A). Although this decrease was not statistically significant, it correlates with the small increase in miR-155 expression observed at this age (Fig. 4A). Furthermore, we observed a decrease in SOCS-1 mRNA levels when miR-155 was overexpressed

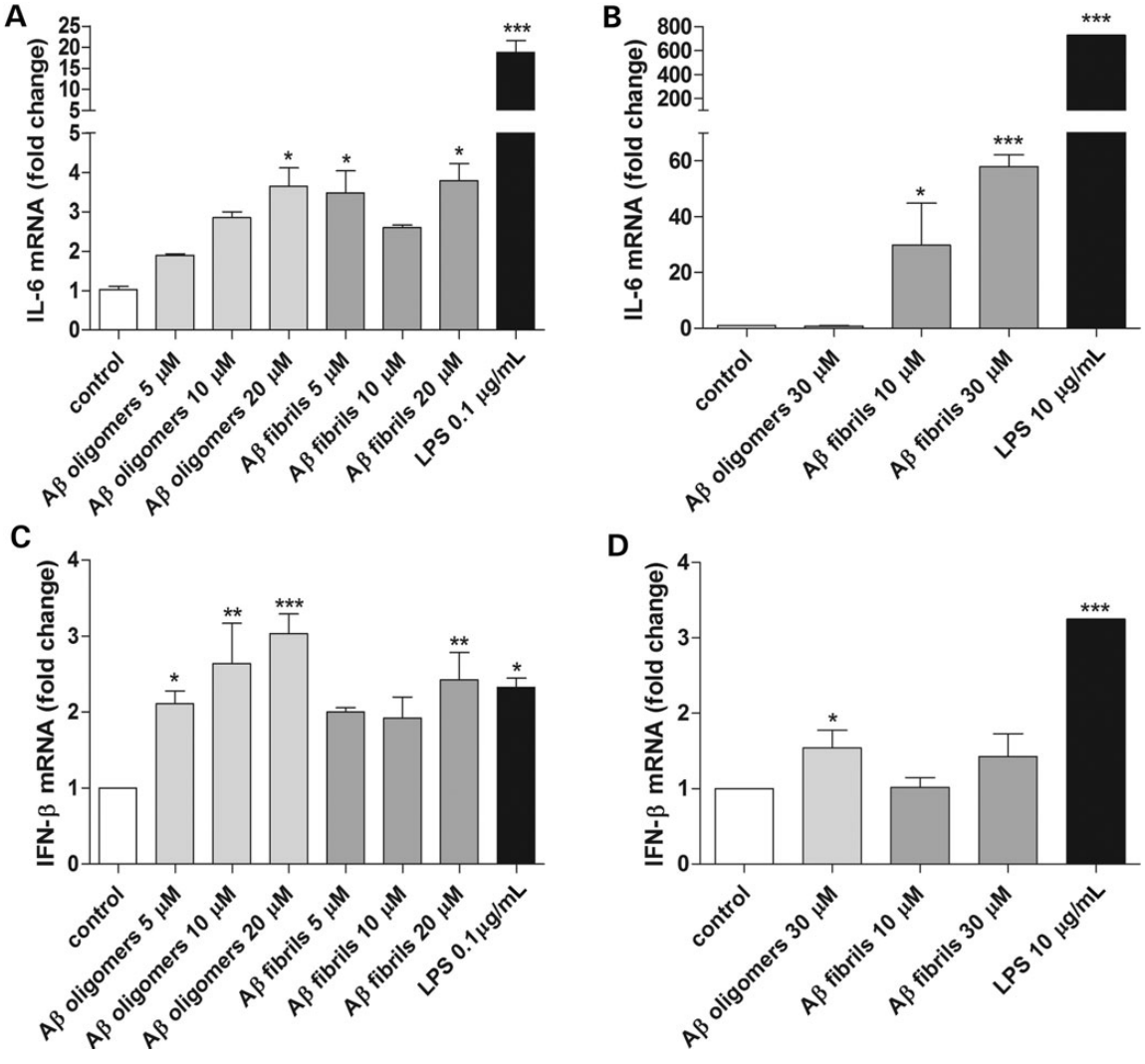

Figure 6. IL-6 and IFN-β expression in Aβ-activated microglia and astrocyte cultures. N9 microglia cells or astrocyte primary cultures were plated and maintained in culture for 1 day before incubation with Aβ oligomers or Aβ fibrils. (**A** and **C**) N9 microglia cells were incubated with 5, 10 and 20 μM, of Aβ for 24 h, while (**B** and **D**) astrocyte primary cultures were incubated with 10 and 30 μM of Aβ for the same period of time. Both cell types were incubated with LPS as a positive control (0.1 μg/ml in microglia and 10 μg/ml in astrocytes). Following the incubation period, total RNA was extracted from each condition and IL-6 and IFN-β levels were quantified by qRT-PCR. Results are expressed as mRNA fold change with respect to control (cells in the absence of stimulus) and are representative of three independent experiments performed in duplicate. $^{*}P < 0.05$, $^{**}P < 0.01$ and $^{***}P < 0.001$with respect to control.

in astrocyte primary cultures and an increase in SOCS-1 mRNA levels when astrocytes were transfected with a LNA-modified oligonucleotide complementary to miR-155 (anti-miR-155) (Supplementary Material, Fig. S6). Thus, we can conclude that in astrocytes, as well as previously shown in microglia, SOCS-1 is a direct target of miR-155 and its expression can be regulated by the levels of this miRNA. Therefore, and taking into consideration the activation of both microglia and astrocytes in 3xTg AD animals, it stands to reason that the observed increase in miR-155 expression in this mouse model is at least partially responsible for the downregulation of SOCS-1.

C-Jun is responsible for miR-155 upregulation in the presence of the Aβ peptide

Although in the context of inflammation, miR-155 upregulation has been addressed multiple times in different pathological settings, the mechanisms regulating miR-155 expression have not been completely elucidated and different authors have proposed the involvement of the JNK or NF-κB signaling pathways in the control of the non-protein coding BIC gene (gene encoding miR-155) (27,45). In order to explore which transcription factor is responsible for the increase in the miR-155 levels observed in 3xTg AD mice, we evaluated the total protein levels of c-Jun, the transcription factor downstream of JNK, and NF-κB in 3xTg AD mice at 3 and 12 months and in their age-matched WT littermates. Western blot analysis revealed an early upregulation of c-Jun levels in 3-month 3xTg AD animals that was still present at 12 months (Fig. 8). As shown, a 2- and 2.5-fold increase in c-Jun expression was observed in 3xTg AD mice at 3 and 12 months, respectively, with respect to WT mice. However, no significant differences were observed in the expression of NF-κB between 3xTg AD and WT mice (Supplementary Material, Fig. S7).

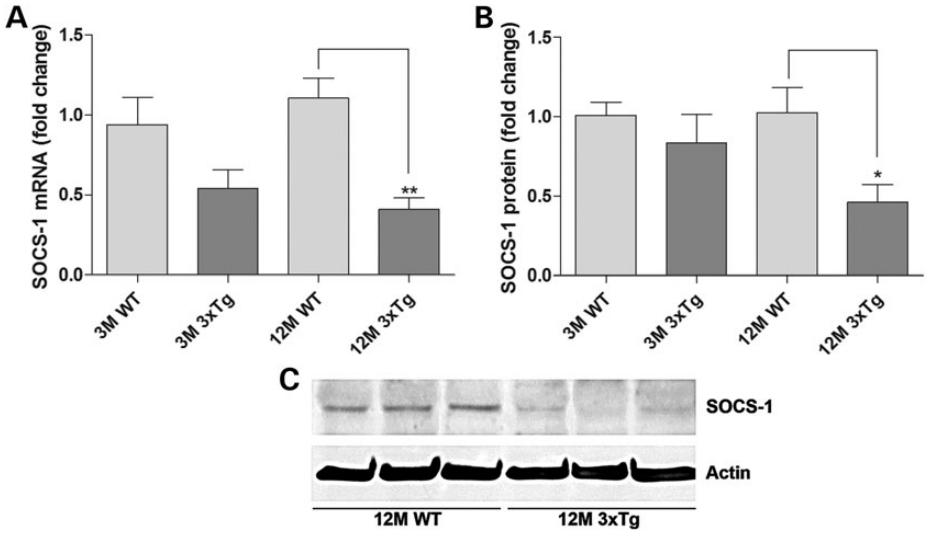

Figure 7. SOCS-1 mRNA and protein levels in 12-month 3xTg AD mice. Protein and RNA extracts of hippocampal and cortical brain regions were obtained from 3xTg AD animals at 3 and 12 months and their age-matched WT littermates. (**A**) SOCS-1 mRNA levels were quantified by qRT-PCR. Results are expressed as mRNA fold change with respect to 3-month WT mice. (**B**) SOCS-1 protein levels were quantified by western blot and are expressed as protein fold change with respect to 3-month WT mice. (**C**) Representative gel showing decreased levels of SOCS-1 in 3xTg AD mice at 12 months compared with age-matched WT littermates. All results are representative of $n = 6$ animals per experimental group. $^{*}P < 0.05$ and $^{**}P < 0.01$ with respect to 12-month WT mice.

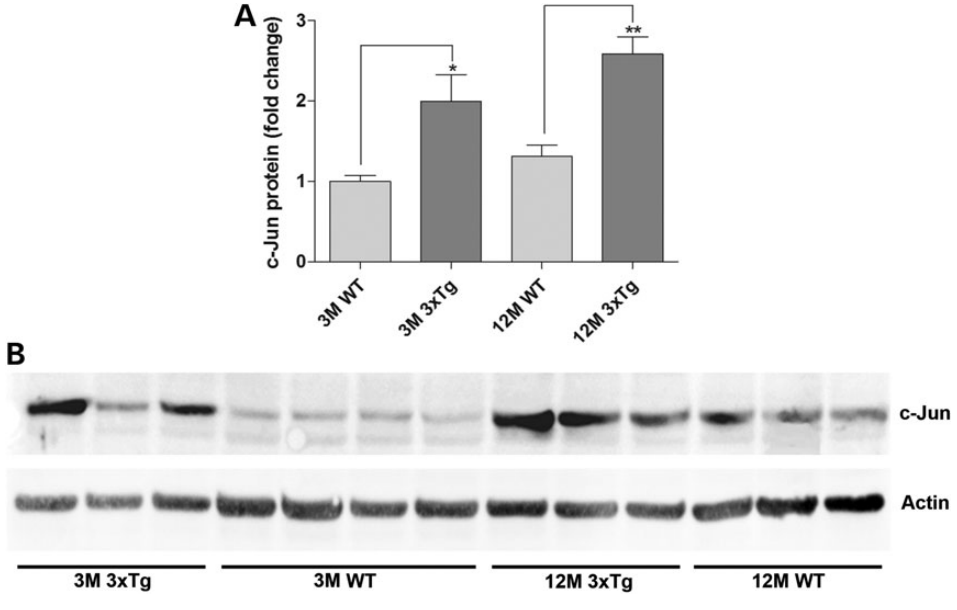

Figure 8. C-Jun expression in 3xTg AD mice. Protein extracts of hippocampal and cortical brain regions were obtained from 3xTg AD animals at 3 and 12 months and their age-matched WT littermates. (**A**) C-Jun protein levels were quantified by western blot and are expressed as protein fold change with respect to 3-month WT mice. (**B**) Representative gel showing increased c-Jun levels in 3xTg AD mice at 3 and 12 months with respect to WT littermates. All results are representative of $n = 6$ animals for each experimental group. $^{*}P < 0.05$ and $^{**}P < 0.01$ compared with age-matched WT littermates.

Based on the results obtained *in vivo* concerning the levels of c-Jun in AD transgenic animals, we hypothesized that this transcription factor could contribute to miR-155 overexpression upon Aβ activation in microglia and astrocytes. In order to test this hypothesis, a siRNA sequence targeting c-Jun (siRNA c-Jun) was used to silence c-Jun translation in N9 microglia cells and astrocyte primary cultures. Twenty-four hours after transfection, both cell types were exposed to Aβ fibrils (20 μM in the case of microglia or 30 μM in astrocytes), since this Aβ species was previously shown to increase miR-155 expression. The levels of this miRNA were evaluated by qRT-PCR and *in situ* hybridization and a siRNA with a scrambled sequence (siRNA Mut) was used as control in this experiment, in order to detect the presence of unspecific effects related with the transfection process *per se*. We observed that in both N9 microglia cells (Fig. 9A) and astrocytes (Fig. 9B), the expression of miR-155 was decreased in cells where c-Jun had been silenced prior to Aβ fibrils exposure, with respect to cells transfected

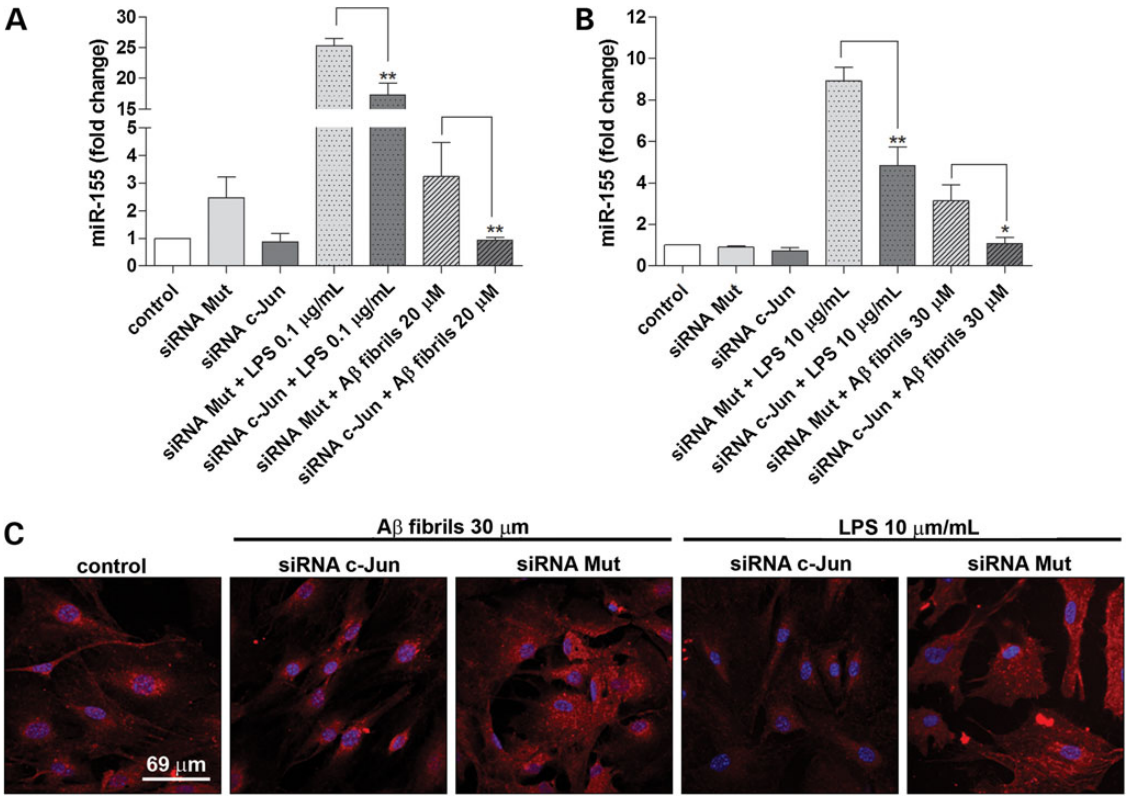

Figure 9. MiR-155 expression in microglia and astrocytes following c-Jun silencing and Aβ exposure. N9 microglia cells and astrocyte primary cultures were plated and maintained in culture for 1 day before cell transfection with anti-c-Jun siRNA (siRNA c-Jun) or a non-targeting siRNA (siRNA Mut) at 50 nM. Four hours after transfection, the cell medium was replaced by fresh RPMI-1640 5% FBS (N9 microglia) or DMEM 10% FBS (astrocytes) and 24 h later, N9 microglia cells were exposed to 20 μM of Aβ fibrils or 0.1 μg/ml of LPS, while primary astrocytes were stimulated with 30 μM of Aβ fibrils or 10 μg/ml of LPS for 24 h. Following this period of time, total RNA was extracted from each condition and miR-155 levels were quantified by qRT-PCR in (**A**) N9 microglia cells or (**B**) astrocytes. Results are expressed as miRNA fold change with respect to control (untransfected cells). (**C**) *In situ* hybridization was used to visualize miR-155 expression in astrocyte cultures. Cells were labeled with a DIG-bound LNA probe specific for miR-155 detection (red), followed by nuclei labeling with Hoechst 33342 (blue). Confocal images from all experimental conditions were acquired with a confocal Zeiss LSM 510 Meta microscope, using the ×60 oil objective. All results are representative of three independent experiments performed in duplicate. $^{*}P < 0.05$ and $^{**}P < 0.01$ with respect to N9 microglia cells or astrocytes transfected with siRNA Mut and exposed to similar stimulus.

with the siRNA Mut. Similar results were observed in parallel experiments performed with cells activated with LPS. Moreover, upon c-Jun silencing, miR-155 expression was similar in Aβ-activated microglia and astrocytes, with respect to transfected or non-transfected non-activated cells. These results were corroborated by *in situ* hybridization studies, which also revealed a significant reduction in miR-155 labeling in astrocyte primary cultures. As can be observed in Figure 9C, the intensity and number of red dots inside astrocytes where c-Jun was silenced prior to cell activation with Aβ fibrils or LPS were much lower than those detected in astrocytes transfected with the siRNA Mut. Since c-Jun silencing *per se* did not reduce miR-155 levels, these findings allowed us to conclude that the observed reduction in miR-155 expression was strictly dependent on cell activation. Although altogether these results do not exclude the contribution of other transcription factors to miR-155 regulation, they strongly suggest that the JNK pathway and its terminal transcription factor c-Jun play an important role in miR-155 upregulation following microglia and astrocyte exposure to Aβ, and unveil the interesting possibility of using an inflammatory approach based on c-Jun silencing to decrease neuroinflammation in the context of AD.

DISCUSSION

Neuroinflammation is a physiological response to brain injury as well as to the accumulation of protein aggregates, which characterizes several neurodegenerative disorders. In the last decade, a number of studies have reported genetic variations in immune-related genes associated with a high risk of Parkinson's disease and AD (46–48) and showed that the products of some of these genes, including inflammatory cytokines and chemokines, have the potential to be used as peripheral biomarkers of AD (49,50). These studies also contributed to clarify, once and for all, the important contribution of the immune response in the context of AD.

Due to the ability of immune-derived brain cells to phagocyte not only foreign organisms but also endogenous particles, some authors have proposed an important role of these cells in regulating the levels of Aβ in the CNS. The expression of key receptors of the innate immune system, such as CD14, TLR2, TLR4 and TLR9, by immune-derived brain cells can be considered as a defense mechanism to prevent Aβ accumulation, since these receptors contribute to the modulation of Aβ fibrillar levels by increasing Aβ uptake by local microglia (51,52). However,

these results must be considered carefully. In this regard, a recent study of *in vivo* two-photon microscopy revealed a strong impairment of microglial function (motility and phagocytic activity) in two different mouse models of AD, which correlated spatially and temporarily with the deposition of Aβ plaques (53). These findings, together with other studies showing a shift of chronic Aβ-exposed microglia to more pro-inflammatory phenotypes (M1) instead of pro-phagocytic phenotypes (M2) (54), suggest that a shift in the type of immune response mediated by these cells in the AD brain may halt the translation into effective Aβ clearance at a certain stage of the disease, and even contribute to disease progression in the long run. Although the importance of immune cells within the CNS is now fully recognized, the question whether their function can be restored to promote a decrease in the amyloid burden remains. We believe that a complete disclosure of the molecular pathways underlying neuroinflammation prior to Aβ plaque deposition will be of utmost importance to resolve this issue.

Recently, the role of Aβ fibrils in neuronal toxicity was challenged and several reports have revealed that other levels of Aβ oligomerization, such as soluble oligomers, can be responsible for the early pathologic events in AD (55), such as early LTP deficits (56). In our experimental model, the 3xTg AD mice, it was possible to identify a pro-inflammatory phenotype of microglia and astrocytes in 12-month-old animals, which preceded the appearance of Aβ deposits in the form of insoluble plaques (Figs 1 and 2). Although glial response to intraneuronal or preplaque Aβ is still poorly understood, in light of the new 'toxic beta-amyloid hypothesis', our results suggest that the activation of glial cells in the 3xTg AD mice is initiated by the accumulation of intraneuronal Aβ, as well as extracellular oligomeric and protofibrillar Aβ, and it may reflect the early stages of disease pathogenesis. These findings corroborate, at least in part, the results of Rebeck *et al.*, who suggested that intracellular Aβ triggers inflammation prior to extracellular Aβ accumulation (57).

In what concerns the molecular outcomes of microglia and astrocyte activation, such as cytokine expression, we observed an upregulation of both IL-6 and IFN-β mRNA levels in 12-month-transgenic animals (Fig. 3). Although these cytokines are described as having opposite effects regarding their immunomodulatory properties, since basal IFN-β expression is essential to trigger a proper inflammatory IL-6 cell response (58), they can be secreted by glia cells simultaneously, and, IL-6 expression in particular, has been observed as a characteristic of Aβ-induced gliosis (59). While recently Zaheer *et al.* (60) observed IL-6 increased expression in 3xTg AD mice at 16 months, we demonstrated that this inflammatory mediator is already elevated at 12 months (Fig. 3). Moreover, our *in vitro* experiments revealed that, when in the presence of Aβ fibrils, glial cells overexpress IL-6 (Fig. 6A and B, Supplementary Material, Fig. S3A and Supplementary Material, Fig. S4A), one of the strongest inflammatory mediators, which is suggestive of an uncontrolled inflammatory response at late stages of Aβ-triggered neuroinflammation. These results are in agreement with the strong upregulation of miR-155 observed in 12-month 3xTg AD mice (Fig. 4A and B) and in microglia or astrocytes following exposure to Aβ fibrils (Fig. 5A and B), since to overexpress an inflammatory cytokine such as IL-6, these cells need to block the activity of SOCS-1, a protein usually responsible for suppressing cytokine expression and a direct target of miR-155.

Our *in vitro* results show that IFN-β, considered to be an immunomodulatory cytokine due to its ability to enhance other cytokine signaling, is more expressed when glial cells are exposed to Aβ oligomers than to Aβ fibrils (Fig. 6C and D, Supplementary Material, Fig. S3C and Supplementary Material, Fig. S4B). This observation suggests that at early stages of Aβ aggregation, microglia and astrocytes try to control neuroinflammation caused by Aβ, which induces the release of cytokines that propagate inflammation throughout the brain. However, the significance of Aβ oligomer-induced IFN-β *in vivo* remains to be fully elucidated. In light of its immunosuppressive nature, IFN-β also induces the expression of SOCS-1 in human primary macrophages and in murine primary microglia, through STAT-1α transcription factor activation, leading to the inhibition of IFN-β signaling in a negative feedback loop (61). However, one of the most described membrane-bound Aβ receptor includes TLR4, and the activation of this receptor induces the expression of miR-155, whose levels are significantly elevated in 3xTg AD mice at 12 months (Fig. 4A and B). Consequently, being a direct target of miR-155, SOCS-1 protein is downregulated at this age (Fig. 7B and C). Based on these results, we suggest that IFN-β signaling is overactivated in AD, since the SOCS-1 negative feedback loop necessary to control IFN-β is abolished due to miR-155 upregulation.

Overall, our results point to an important contribution of miR-155 upregulation, and consequent SOCS-1 downregulation, to the immune response triggered by excessive production of the Aβ peptide in AD. Since miR-155 expression has been largely associated with the maintenance of a pro-inflammatory M1 phenotype in both macrophages and microglia (26,41) our findings also corroborate the hypothesis that prolonged exposure to Aβ peptide may promote chronic neuroinflammation, thus contributing to disease progression. In light of these results, we consider that miR-155 can constitute an interesting and promising molecular target in AD. Recently, our group has developed targeted stable nucleic acid lipid particles (SNALPs) that exhibit excellent features for systemic *in vivo* administration of LNAs in order to modulate miRNA expression in the brain (62). This strategy could be explored in the context of AD by targeting glia cells with the purpose of decreasing the levels of miR-155.

It is known that miR-155 is encoded within the BIC gene and its expression can be induced in response to LPS and other TLR ligands, such as poly(I:C), IFN-β or TNF-α, and in negative feedback loops associated with miR-155 direct targets, such as transcription factors c/ebp Beta (63) and PU.1 (64). Nevertheless, miR-155 regulation processes are still relatively unknown, especially in a disease context. Some studies have suggested that miR-155 is induced after NF-κB activation (45), but other transcription factors have also been associated with the expression of the primary transcript BIC, including the transcription factor AP-1 (27), which is composed of homo- or heterodimers of c-Jun and c-Fos. The results obtained in our study indicate that, in the context of AD, miR-155 expression is regulated, at least in part, by the c-Jun transcription factor (Fig. 9). Moreover, this study revealed that this transcription factor, but not NF-κB, is upregulated at an early time point in this AD animal model (3-month 3xTg AD mice) (Fig. 8), long before Aβ extracellular deposition in the nervous tissue, suggesting a possible relation between c-Jun upregulation and intracellular Aβ production.

Of note, c-Jun has also been previously shown to be an important regulator of Aβ-induced neuronal apoptosis (17). Importantly, in this work, we disclosed another function of c-Jun, which takes place prior to neuronal death and is related with the regulation of Aβ-associated inflammation in microglia and astrocytes. Taking into consideration these results and our previous work on c-Jun contribution to acute excitotoxic lesion, which showed that c-Jun silencing using siRNAs was able to reduce neuronal loss and microglia activation in the hippocampus (20), we propose that a similar silencing strategy can also be applied to control neuroinflammation at early stages of AD.

MATERIALS AND METHODS

Materials

The anti-miR-155 locked nucleic acid *in situ* hybridization probe as well as the quantitative reverse transcription (qRT) PCR primers for detection and determination of miR-155 were obtained from Exiqon (Vedbaek, Denmark). The qRT-PCR primers for mRNA quantification were purchased from Qiagen (Hilden, Germany). The anti-c-Jun siRNA (5′-AGTCATGAACCACGTTAAC-3′) (siRNA c-Jun) and the non-silencing siRNA (siRNA Mut) used as control were purchased from Shangai GenePharma (Shanghai, P.R. China). The Lipofectamine™ RNAiMAX Transfection Reagent was purchased from Invitrogen (Carlsbad, CA, USA). The ionized calcium-binding adapter molecule 1 (IBA-1) antibody for immunohistochemistry was obtained from Wako Pure Chemical Industries, Ltd. (Osaka, Japan) and the GFAP and Aβ antibodies were purchased from Chemicon International, Inc. (Temecula, CA, USA). The SOCS-1 and the c-Jun antibodies for western blot were purchased from Cell Signaling (Danvers, MA, USA) and the actin antibody was obtained from Sigma (Saint Louis, MO, USA). The $A\beta_{1\text{-}42}$ peptide was obtained from American Peptide (Sunnyvale, CA, USA). All the other chemicals were obtained from Sigma, unless stated otherwise.

Animals

All efforts were made to minimize suffering and the number of animals used in this study, according to the guidelines of the Portuguese National Authority for Animal Health. The AD triple transgenic animals (3xTg AD mice) were obtained from Dr Frank LaFerla laboratory at the Department of Neurobiology and Behaviour and Institute for Brain Aging and Dementia, University of California at Irvine. The animals were found to have the same phenotypic and behavioral characteristics, as previously described by Dr Frank LaFerla group (32,56). Briefly, human APP cDNA harboring the Swedish double mutation (KM670/671NL) and human four-repeat tau harboring the P301L mutation were co-microinjected into single-cell embryos of homozygous $PS1_{M146V}$ knock-in mice. The PS1 mice were originally generated on a hybrid 129/C57BL6 background (65). The animals ($n = 6$ for each experimental group) were maintained under controlled light and environmental conditions (12 h dark/light cycle, 23 ± 1°C, 55 ± 5% relative humidity), having free access to food and water. Age- and gender-matched non-transgenic animals were used as controls. The animals were killed at 3 or 12 months of age and the brains were removed following transcardial perfusion with 20 ml of an ice-cold 0.9% NaCl solution. One hemisphere of each brain was post-fixed (12 h) in a fixative solution of 4% paraformaldehyde in 0.9% NaCl, and was kept for 2–3 days in a cryoprotective solution containing 25% sucrose. After this period, the brain hemisphere was dried and frozen at −80°C until further use. The other hemisphere was used for protein and mRNA extraction. For this purpose, the hemisphere was placed on an acrylic matrix and a 4 mm coronal section was cut with a stainless steel razor. The hippocampal and cortical regions from this section were dissected and kept at −80°C until protein or mRNA extraction.

Immunohistochemistry

Immunohistochemistry of brain slices was performed as described previously (66). Briefly, coronal sections of 30 μm were cut throughout the entire cortex and hippocampus at −20°C in a cryostat (Leica CM 3050 S, Leica, Wetzlar, Germany) and stored in 48-well multiwell plates in PBS supplemented with 0.05 mM sodium azide at 4°C until immunohistochemical processing. Free-floating sections were permeabilized for 2 h with 0.1% Triton X-100 containing 10% normal goat serum (Gibco, Life Technologies, Carlsbad, CA, USA) at room temperature, followed by incubation with the primary antibodies against IBA-1 (1:1000), GFAP (1:1000) or Aβ (1:2000) in blocking solution, overnight at 4°C. Sections were then washed three times and incubated for 2 h at room temperature with the respective biotinylated antibodies (Vector Laboratories, Burlingame, CA, USA). Bound antibodies were visualized using the VECTASTAIN® ABC kit, with 3,3′-diaminobenzidine tetrahydrochloride (DAB metal concentrate; Pierce) (Thermo Fisher Scientific, Rockford, IL, USA) as substrate. After washed three times, the sections were mounted in FluorSave™ Reagent (Calbiochem, Merk Millipore, Billerica, MA, USA) on microscope slides. All slices were observed by visible immunostaining, under a Zeiss Axiovert microscope (Carl Zeiss Microimaging), equipped with AxioCam HR color digital cameras (Carl Zeiss Microimaging) using ×5, ×20 and ×40 objectives.

Microglia and astrocyte cell culture

N9 microglia cells (immortalized mouse microglia cells) were cultured at 37°C in a humidified atmosphere containing 5% CO_2 and maintained in RPMI-1640 medium (Gibco, Life Technologies) supplemented with 5% heat-inactivated fetal bovine serum (FBS), 100 μg/ml streptomycin and 1 U/ml penicillin. N9 microglia cells were plated 24 h before the beginning of each experiment at a density of 100 000 cells/well in uncoated 12-well multiwell plates for RNA extraction.

Astrocyte primary cultures were prepared from 3-day-old C57/BL6 newborn mice. After digestion and dissociation of the dissected mouse cortices in HBSS solution (Hank's Buffered Salt Solution, 136.7 mM NaCl, 2.1 mM $NaHCO_3$, 0.22 μM KH_2PO_4, 5.3 mM KCl, 2.7 mM glucose, 10 mM HEPES, pH 7.3) supplemented with 0.25% trypsin, 0.001% DNase I and 10 μg/ml gentamicin, mixed glial cultures were prepared by resuspending the cell suspension in DMEM medium (10 mM $NaHCO_3$, 25 mM HEPES, 10 μg/ml gentamicin, pH 7.3) containing 10% FBS (Gibco, Life Technologies). Cells were seeded on 75 cm^2

flasks at a density of 3×10^6 cells per flask and maintained in the culture flasks for 10 days at 37°C in a humidified atmosphere containing 5% CO_2, with medium changes each 2–3 days. When the mixed glial cultures achieved 70% confluence, microglia and oligodendrocytes attached at the upper layer of the astrocyte culture were detached by shaking for 4 h in an orbital shaker at 220 rpm and 37°C. The purified astrocytes were trypsinized and plated in DMEM 10% FBS medium at a density 240 000 cells/well in uncoated 6-well multiwell plates for RNA extraction, at a density of 100 000 cells/well in 12-well multiwell plates for cell transfection and fluorescence microscopy experiments and at 20 000 cells/well in microslide eight-well ibiTreat chamber slides (ibidi, Germany) for *in situ* hybridization experiments. In all cases, after shaking, astrocytes were maintained in culture for 3 days before the beginning of the experiments. Regular characterization of primary astrocyte cultures by GFAP and CD11b immunostaining indicated the presence of over 97% astrocytes, confirming the purity of these cultures.

Preparation of amyloid-β (Aβ) oligomers and fibrils for microglia and astrocytes treatment

$A\beta_{1-42}$ oligomers and fibrils were prepared as previously described (67). Briefly, synthetic $A\beta_{1-42}$ peptide (American Peptides) was dissolved in 1,1,1,3,3,3-hexafluoro-2-propanol (HFIP) to obtain a 1 mM solution. The HFIP was then evaporated in a Speed Vac (Ílshin Laboratory. Co., Ltd., Ede, the Netherlands) and the dried peptide was resuspended in anhydrous dimethyl sulfoxide (DMSO) at a 5 mM solution. $A\beta_{1-42}$ oligomers were prepared by diluting the $A\beta_{1-42}$ solution in Phenol Red-free Ham's F-12 medium without glutamine to a 100 μM final concentration and incubated overnight at 4°C. The solution was then centrifuged at 15 000*g* for 10 min at 4°C to remove insoluble aggregates, and the supernatant, containing soluble oligomers, was transferred to clean tubes and stored at 4°C. $A\beta_{1\text{-}42}$ fibrils were prepared by diluting the 5 mM $A\beta_{1-42}$ solution in DMSO to a concentration of 200 μM in 100 mM HEPES buffer (pH 7.5) and aged at 37°C for 7 days. The preparation was then centrifuged during 10 min at 15 000*g* at room temperature and the supernatant, containing soluble oligomers, was discarded. The pellet containing Aβ fibrils (and possibly protofibrils) was resuspended in 100 mM HEPES buffer (pH 7.5). Protein concentrations of Aβ oligomers and fibrils were determined using the Bio-Rad Dc protein dye assay reagent.

The presence of different assembly forms (monomers, oligomers and fibrils) of $A\beta_{1-42}$ in the different preparations and the purity of isolated oligomers and fibrils were evaluated by gel electrophoresis (Supplementary Material, Fig. S8). Aβ samples containing 10 μg of protein were diluted (1:2) with sample buffer (40% (w/v) glycerol, 2% (w/v) SDS, 0.2 M Tris–HCl, pH 6.8 and 0.005% (w/v) Coomassie G-250) and were separated by electrophoresis on a 4–16% Tris–Tricine SDS gel. Samples were not boiled to minimize disaggregation prior to electrophoresis. To facilitate the identification of proteins, a Low-Range Rainbow protein standard was used. The gel was stained with Coomassie G-250 for 10 min, followed by overnight incubation with a destaining solution composed of 10% acetic acid and 30% methanol in H_2O. Analysis of band weight was performed using the Quantity One software (Bio-Rad, Hercules, CA, USA) and the percentage of the Aβ aggregation forms in each Aβ preparation is presented in the Supplementary Material, Table S1.

In order to accomplish Aβ-mediated cell activation, N9 microglia cells were treated with Aβ oligomers or fibrils at a 5, 10 and 20 μM concentration and astrocytes were treated with 10 and 30 μM Aβ oligomers or fibrils for 24 h. Alternatively, as a positive activation control, N9 microglia cells and astrocytes were incubated with LPS at 0.1 and 10 μg/ml concentrations, respectively.

Transfection experiments

The delivery of siRNAs (siRNA c-Jun or siRNA Mut) to N9 microglia cells and astrocytes was performed using the Lipofectamine™ RNAiMAX Transfection Reagent, according to the manufacturer's instructions (Invitrogen). Briefly, Lipofectamine™ RNAiMAX Transfection Reagent in an Optimem (modification of Eagle''s Minimum Essential Media, 28.5 mM $NaHCO_3$) volume of 50 μl/well was mixed with the appropriate volume of siRNA stock solution to achieve a final siRNA concentration of 50 nM in each well. The mixture was further incubated for 30 min, at room temperature. For qRT-PCR experiments, immediately before transfection, cells were washed and the medium was replaced with Optimem for N9 microglia or DMEM supplemented with 5% FBS for astrocytes (950 μl/well). For fluorescence *in situ* hybridization experiments, astrocytes were plated in μ-slide eight-well ibiTreat chamber slides (ibidi) and transfected in a final volume of 200 μl/well in DMEM 5% FBS. For both qRT-PCR and *in situ* hybridization experiments, after a 4 h transfection period, the cell medium was replaced with fresh DMEM with 10% FBS, in the case of astrocyte cultures, or RPMI-1640 with 5% FBS in N9 microglia cells. Twenty-four hours after transfection, N9 microglia cells were exposed to 0.1 μg/ml LPS or 20 μM Aβ fibrils and primary astrocytes were exposed to 10 μg/ml LPS or 30 μM Aβ fibrils for 24 h. Following this incubation period, RNA extraction and *in situ* hybridization experiments were performed.

Quantitative real-time PCR

Total RNA, including small RNA species, was extracted from brain tissue of 3xTg AD and WT animals with 3 or 12 months, primary astrocyte cultures and N9 microglia cells using the miRCURY Isolation Kit Cells (Exiqon), according to the manufacturer's recommendations for cultured cells. Briefly, after cell lysis, the total RNA was adsorbed to a silica matrix, washed with the recommended buffers and eluted with 35 μl RNase-free water by centrifugation. After RNA quantification, cDNA conversion for miRNA quantification was performed using the Universal cDNA Synthesis Kit (Exiqon). For each sample, cDNA for miRNA detection was produced from 20 ng total RNA according to the following protocol: 60 min at 42°C followed by heat-inactivation of the reverse transcriptase for 5 min at 95°C. The cDNA was diluted 80× with RNase-free water before quantification by qRT-PCR. Synthesis of cDNA for mRNA quantification was performed using the iScript cDNA Synthesis Kit (Bio-Rad) and employing 1 μg total RNA for each reaction, by applying the following protocol: 5 min at 25°C, 30 min at 42°C and 5 min at 85°C. Finally, the cDNA was diluted 1:10 with RNase-free water.

Quantitative PCR was performed in a iQ5 thermocycler (Bio-Rad), using 96-well microtitre plates. The miRCURY LNA™ Universal RT microRNA PCR system (Exiqon) was used in combination with pre-designed LNA primers (Exiqon) for miR-155 and SNORD 110 (reference gene) quantification. A master mix was designed for each primer set and, for each reaction, 12 μl of the master mix were added to 8 μl of cDNA template. All reactions were performed in duplicate at a final volume of 20 μl per well, using the iQ5 Optical System Software (Bio-Rad). The reaction conditions consisted of polymerase activation/denaturation and well-factor determination at 95°C for 10 min, followed by 40 amplification cycles at 95°C for 10 s and 65°C for 1 min (ramp-rate 1.6°C/s).

mRNA quantification was performed using the iQ SYBR Green Supermix Kit (Bio-Rad). The primers for the target genes (SOCS-1, IL-6 and IFN-β) and for the reference gene (HPRT) were pre-designed by Qiagen (QuantiTect Primer, Qiagen, Hilden, Germany). A master mix was prepared for each primer set, containing a fixed volume of SYBR Green Supermix and the appropriate amount of each primer to yield a final concentration of 150 nM. For each reaction, 20 μl master mix was added to 5 μl template cDNA. All reactions were performed in duplicate (two cDNA reactions per RNA sample) at a final volume of 25 μl per well, using the iQ5 Optical System Software (Bio-Rad). The reaction conditions consisted of enzyme activation and well-factor determination at 95°C for 1 min and 30 s, followed by 40 cycles at 95°C for 10 s (denaturation), 30 s at 55°C (annealing), and 30 s at 72°C (elongation).

For both miRNA and mRNA quantification, a melting curve protocol was started immediately after amplification and consisted of 1 min heating at 55°C followed by 80 steps of 10 s, with a 0.5°C increase at each step. Threshold values for threshold cycle determination (*Ct*) were generated automatically by the iQ5 Optical System Software. The miRNA and mRNA fold increase or fold decrease, with respect to control samples, was determined by the Pfaffl method, taking into consideration the different amplification efficiencies of the different genes and miRNAs. The amplification efficiency of each target or reference RNA was determined according to the formula: $E = 10^{(-1/S)} - 1$, where S is the slope of the obtained standard curve.

In situ hybridization

Fluorescence *in situ* hybridization was performed in brain slices of 3xTg AD animals and WT littermates and in primary astrocytes, as described by Lu and Tsourkas (68), with some modifications. Briefly, free-floating brain slices were mounted in microscope slides, washed with PBS, fixed with 4% paraformaldehyde for 30 min at room temperature and permeabilized at 4°C in 70% ethanol for 4 h. Slices were then incubated with fresh acetylation solution [0.1 M triethanolamine and 0.5% (v/v) acetic anhydride] for 30 min at room temperature, rinsed twice in Tris-buffered saline (TBS) and pre-hybridized in the absence of the LNA probe in hybridization buffer [50% formamide, 5× SSC, 5× Denhardt's solution, 250 μg/ml yeast tRNA, 500 μg/ml salmon sperm DNA, 2% (w/v) blocking reagent, 0.1% CHAPs, 0.5% Tween] for 2 h at a temperature 22–25°C below the melting temperature of the probe. The hybridization step was carried out upon overnight incubation at the same temperature with DIG-labelled (digoxigenin-labelled) LNA probes for miR-155. A scrambled probe (negative control) and U6snRNA (positive control) were also used in this experiment (data not shown). Three stringency washes were performed at the same temperature used for probe hybridization to completely remove the non-hybridized probe. Endogenous peroxidase activity was inactivated by incubation in 3% hydrogen peroxide in TBS with 0.1% Tween-20 (TBS-T) for 30 min, followed by three washes with TBS-T. The slides were then placed in blocking solution (TBS-T, 10% heat-inactivated goat serum, 0.5% blocking agent) for 1 h at room temperature and incubated for the same period of time with an anti-DIG antibody (Roche, Amadora, Portugal) conjugated with the hydrogen peroxidase. To amplify the antibody signal, slides were further incubated with a TSA plus Cy3 (PerkinElmer, Waltham, MA) solution for 10 min in the dark, in accordance with the manufacturer's protocol. The slides were finally stained with the fluorescent DNA-binding dye Hoechst 33342 (Invitrogen Life Technologies, Paisley, UK) (1 μg/ml) for 5 min in the dark, washed with cold PBS, and mounted in Mowiol (Fluka; Sigma).

For astrocyte *in situ* hybridization experiments, cells were seeded onto microslide eight-well ibiTreat chamber slides (ibidi) appropriate for confocal microscopy imaging. Following transfection with siRNAs and treatment with LPS, Aβ oligomers or Aβ fibrils, cells were treated as described above.

Confocal images were acquired in a point scanning confocal microscope Zeiss LSM 510 Meta (Zeiss, Göttingen, Germany), with a ×60 oil objective. Digital images were acquired using the LSM 510 META software. All instrumental parameters pertaining to fluorescence detection and image analyses were held constant to allow sample comparison.

Western blot

Total protein extracts were obtained from brain extracts collected from the cortex and hippocampus of 3xTg AD mice and their WT littermates. Briefly, tissue samples were homogenized at 4°C in lysis buffer (50 mM NaCl, 50 mM EDTA, 1% Triton X-100) supplemented with a protease inhibitor cocktail (Roche), 10 μg/ml dithiothreitol and 1 mM PMSF. Protein content was determined using the Bio-Rad Dc protein assay (Bio-Rad). Thirty micrograms of total protein were resuspended in loading buffer (20% glycerol, 10% SDS and 0.1% bromophenol blue), incubated for 5 min at 95°C and loaded into a 10% polyacrylamide gel. After electrophoresis, the proteins were blotted onto a PVDF membrane according to standard protocols and blocked in 5% non-fat milk, before being incubated with the appropriate primary antibody (anti-c-Jun 1:1000 or anti-SOCS1 1:500) overnight at 4°C, and with the appropriate secondary antibody (1:20 000) (GE Healthcare, Waukesha, WI, USA) for 2 h at room temperature. The membranes were then washed several times with saline buffer (TBS-T—25 mM Tris–HCl, 150 mM NaCl, 0.1% Tween) and incubated with ECF (enhanced chemifluorescence substrate - 20 μl/cm^2 of membrane) for 5 min at room temperature. ECF detection was performed using a Molecular Imager Versa Doc MP 4000 System (Bio-Rad) and, for each membrane, the analysis of band intensity was performed using the Quantity One Software (Bio-Rad). Equal protein loading was shown by re-probing the membrane with anti-actin (1:20 000) or anti-tubulin (1:10 000) antibodies and with the appropriate secondary antibody.

Statistical analysis

All data are presented as mean ± standard deviation (SD) and are the result of at least three independent experiments performed in duplicate for *in vitro* studies or $n = 6$ for *in vivo* studies. One-way analysis of variance combined with Tukey's or Dunnett's multiple comparison tests were used for multiple comparisons in all experiments. Statistical differences are presented as probability levels of $P < 0.05$ (*), $P < 0.01$ (**) and $P < 0.001$ (***). Calculations were performed with a standard statistical software (GraphPad Prism 5).

SUPPLEMENTARY MATERIAL

Supplementary Material is available at HMG online.

ACKNOWLEDGEMENTS

The authors would like to acknowledge the groups of Professor Cristina Rego and Dr John Jones, from the Center for Neuroscience and Cell Biology of the University of Coimbra, particularly to Gladys Caldeira and Filipa Simões, for their help regarding the preparation of Aβ oligomers and Aβ fibrils. The authors would also like to acknowledge the Doctoral Programme in Experimental Biology and Biomedicine of the Center for Neuroscience and Cell Biology, University of Coimbra.

Conflict of Interest statement. None declared.

FUNDING

This work was supported by the Portuguese Foundation for Science and Technology (FCT) and FEDER/COMPETE (PTDC/BIM-MEC/0651/2012) and PEst-C/SAU/LA0001/2013-2014. J.R.G. is a recipient of a fellowship from FCT (SFRH/BD/51677/2011).

REFERENCES

1. El Khoury, J. and Luster, A.D. (2008) Mechanisms of microglia accumulation in Alzheimer's disease: therapeutic implications. *Trends Pharmacol. Sci.*, **29**, 626–632.
2. Dheen, S.T., Jun, Y., Yan, Z., Tay, S.S. and Ling, E.A. (2005) Retinoic acid inhibits expression of TNF-alpha and iNOS in activated rat microglia. *Glia*, **50**, 21–31.
3. Lucin, K.M. and Wyss-Coray, T. (2009) Immune activation in brain aging and neurodegeneration: too much or too little? *Neuron*, **64**, 110–122.
4. Glass, C.K., Saijo, K., Winner, B., Marchetto, M.C. and Gage, F.H. (2010) Mechanisms underlying inflammation in neurodegeneration. *Cell*, **140**, 918–934.
5. El Khoury, J., Toft, M., Hickman, S.E., Means, T.K., Terada, K., Geula, C. and Luster, A.D. (2007) Ccr2 deficiency impairs microglial accumulation and accelerates progression of Alzheimer-like disease. *Nat. Med.*, **13**, 432–438.
6. Wyss-Coray, T., Loike, J.D., Brionne, T.C., Lu, E., Anankov, R., Yan, F., Silverstein, S.C. and Husemann, J. (2003) Adult mouse astrocytes degrade amyloid-beta in vitro and in situ. *Nat. Med.*, **9**, 453–457.
7. D'Andrea, M.R., Cole, G.M. and Ard, M.D. (2004) The microglial phagocytic role with specific plaque types in the Alzheimer disease brain. *Neurobiol. Aging*, **25**, 675–683.
8. Griffin, W.S., Sheng, J.G., Royston, M.C., Gentleman, S.M., McKenzie, J.E., Graham, D.I., Roberts, G.W. and Mrak, R.E. (1998) Glial-neuronal interactions in Alzheimer's disease: the potential role of a 'cytokine cycle' in disease progression. *Brain Pathol.*, **8**, 65–72.
9. Parachikova, A., Agadjanyan, M.G., Cribbs, D.H., Blurton-Jones, M., Perreau, V., Rogers, J., Beach, T.G. and Cotman, C.W. (2007) Inflammatory changes parallel the early stages of Alzheimer disease. *Neurobiol. Aging*, **28**, 1821–1833.
10. Saijo, K., Winner, B., Carson, C.T., Collier, J.G., Boyer, L., Rosenfeld, M.G., Gage, F.H. and Glass, C.K. (2009) A Nurr1/CoREST pathway in microglia and astrocytes protects dopaminergic neurons from inflammation-induced death. *Cell*, **137**, 47–59.
11. Agulhon, C., Sun, M.Y., Murphy, T., Myers, T., Lauderdale, K. and Fiacco, T.A. (2012) Calcium Signaling and Gliotransmission in Normal versus Reactive Astrocytes. *Front. Pharmacol.*, **3**, 139.
12. Heneka, M.T. and O'Banion, M.K. (2007) Inflammatory processes in Alzheimer's disease. *J. Neuroimmunol.*, **184**, 69–91.
13. Walter, S., Letiembre, M., Liu, Y., Heine, H., Penke, B., Hao, W., Bode, B., Manietta, N., Walter, J., Schulz-Schuffer, W. *et al.* (2007) Role of the toll-like receptor 4 in neuroinflammation in Alzheimer's disease. *Cell Physiol. Biochem.*, **20**, 947–956.
14. Letiembre, M., Liu, Y., Walter, S., Hao, W., Pfander, T., Wrede, A., Schulz-Schaeffer, W. and Fassbender, K. (2009) Screening of innate immune receptors in neurodegenerative diseases: a similar pattern. *Neurobiol. Aging*, **30**, 759–768.
15. Stewart, C.R., Stuart, L.M., Wilkinson, K., van Gils, J.M., Deng, J., Halle, A., Rayner, K.J., Boyer, L., Zhong, R., Frazier, W.A. *et al.* (2010) CD36 ligands promote sterile inflammation through assembly of a Toll-like receptor 4 and 6 heterodimer. *Nat. Immunol.*, **11**, 155–161.
16. Gorina, R., Font-Nieves, M., Marquez-Kisinousky, L., Santalucia, T. and Planas, A.M. (2011) Astrocyte TLR4 activation induces a proinflammatory environment through the interplay between MyD88-dependent NFkappaB signaling, MAPK, and Jak1/Stat1 pathways. *Glia*, **59**, 242–255.
17. Tang, S.C., Lathia, J.D., Selvaraj, P.K., Jo, D.G., Mughal, M.R., Cheng, A., Siler, D.A., Markesbery, W.R., Arumugam, T.V. and Mattson, M.P. (2008) Toll-like receptor-4 mediates neuronal apoptosis induced by amyloid beta-peptide and the membrane lipid peroxidation product 4-hydroxynonenal. *Exp. Neurol.*, **213**, 114–121.
18. Bernardi, A., Frozza, R.L., Meneghetti, A., Hoppe, J.B., Battastini, A.M., Pohlmann, A.R., Guterres, S.S. and Salbego, C.G. (2012) Indomethacin-loaded lipid-core nanocapsules reduce the damage triggered by Abeta1–42 in Alzheimer's disease models. *Int. J. Nanomed.*, **7**, 4927–4942.
19. Vukic, V., Callaghan, D., Walker, D., Lue, L.F., Liu, Q.Y., Couraud, P.O., Romero, I.A., Weksler, B., Stanimirovic, D.B. and Zhang, W. (2009) Expression of inflammatory genes induced by beta-amyloid peptides in human brain endothelial cells and in Alzheimer's brain is mediated by the JNK-AP1 signaling pathway. *Neurobiol. Dis.*, **34**, 95–106.
20. Cardoso, A.L., Costa, P., de Almeida, L.P., Simoes, S., Plesnila, N., Culmsee, C., Wagner, E. and de Lima, M.C. (2010) Tf-lipoplex-mediated c-Jun silencing improves neuronal survival following excitotoxic damage in vivo. *J. Control. Release*, **142**, 392–403.
21. Lukiw, W.J., Zhao, Y. and Cui, J.G. (2008) An NF-kappaB-sensitive micro RNA-146a-mediated inflammatory circuit in Alzheimer disease and in stressed human brain cells. *J. Biol. Chem.*, **283**, 31315–31322.
22. Cogswell, J.P., Ward, J., Taylor, I.A., Waters, M., Shi, Y., Cannon, B., Kelnar, K., Kemppainen, J., Brown, D., Chen, C. *et al.* (2008) Identification of miRNA changes in Alzheimer's disease brain and CSF yields putative biomarkers and insights into disease pathways. *J. Alzheimers Dis.*, **14**, 27–41.
23. Li, Y.Y., Cui, J.G., Dua, P., Pogue, A.I., Bhattacharjee, S. and Lukiw, W.J. (2011) Differential expression of miRNA-146a-regulated inflammatory genes in human primary neural, astroglial and microglial cells. *Neurosci. Lett.*, **499**, 109–113.
24. Thai, T.H., Calado, D.P., Casola, S., Ansel, K.M., Xiao, C., Xue, Y., Murphy, A., Frendewey, D., Valenzuela, D., Kutok, J.L. *et al.* (2007) Regulation of the germinal center response by microRNA-155. *Science*, **316**, 604–608.
25. Cardoso, A.L., Guedes, J.R., Pereira de Almeida, L. and Pedroso de Lima, M.C. (2012) miR-155 modulates microglia-mediated immune response by down-regulating SOCS-1 and promoting cytokine and nitric oxide production. *Immunology*, **135**, 73–88.
26. Guedes, J., Cardoso, A.L. and Pedroso de Lima, M.C. (2013) Involvement of microRNA in microglia-mediated immune response. *Clin. Dev. Immunol.*, **2013**, 186872.
27. O'Connell, R.M., Taganov, K.D., Boldin, M.P., Cheng, G. and Baltimore, D. (2007) MicroRNA-155 is induced during the macrophage inflammatory response. *Proc. Natl. Acad. Sci. USA*, **104**, 1604–1609.

28. Onyeagucha, B.C., Mercado-Pimentel, M.E., Hutchison, J., Flemington, E.K. and Nelson, M.A. (2013) S100P/RAGE signaling regulates microRNA-155 expression via AP-1 activation in colon cancer. *Exp. Cell Res.*, **319**, 2081–2090.
29. Mor, E., Cabilly, Y., Goldshmit, Y., Zalts, H., Modai, S., Edry, L., Elroy-Stein, O. and Shomron, N. (2011) Species-specific microRNA roles elucidated following astrocyte activation. *Nucleic Acids Res.*, **39**, 3710–3723.
30. Tarassishin, L., Bauman, A., Suh, H.S. and Lee, S.C. (2012) Anti-viral and anti-inflammatory mechanisms of the innate immune transcription factor interferon regulatory factor 3: relevance to human CNS diseases. *J. Neuroimmune Pharmacol.*, **8**, 132–144.
31. McGeer, E.G. and McGeer, P.L. (2003) Inflammatory processes in Alzheimer's disease. *Prog. Neuropsychopharmacol. Biol. Psychiatry*, **27**, 741–749.
32. Oddo, S., Caccamo, A., Kitazawa, M., Tseng, B.P. and LaFerla, F.M. (2003) Amyloid deposition precedes tangle formation in a triple transgenic model of Alzheimer's disease. *Neurobiol. Aging*, **24**, 1063–1070.
33. Janelsins, M.C., Mastrangelo, M.A., Oddo, S., LaFerla, F.M., Federoff, H.J. and Bowers, W.J. (2005) Early correlation of microglial activation with enhanced tumor necrosis factor-alpha and monocyte chemoattractant protein-1 expression specifically within the entorhinal cortex of triple transgenic Alzheimer's disease mice. *J. Neuroinflammation*, **2**, 23.
34. Janelsins, M.C., Mastrangelo, M.A., Park, K.M., Sudol, K.L., Narrow, W.C., Oddo, S., LaFerla, F.M., Callahan, L.M., Federoff, H.J. and Bowers, W.J. (2008) Chronic neuron-specific tumor necrosis factor-alpha expression enhances the local inflammatory environment ultimately leading to neuronal death in 3xTg-AD mice. *Am. J. Pathol.*, **173**, 1768–1782.
35. Pennanen, C., Kivipelto, M., Tuomainen, S., Hartikainen, P., Hanninen, T., Laakso, M.P., Hallikainen, M., Vanhanen, M., Nissinen, A., Helkala, E.L. *et al.* (2004) Hippocampus and entorhinal cortex in mild cognitive impairment and early AD. *Neurobiol. Aging*, **25**, 303–310.
36. Tili, E., Michaille, J.J., Cimino, A., Costinean, S., Dumitru, C.D., Adair, B., Fabbri, M., Alder, H., Liu, C.G., Calin, G.A. *et al.* (2007) Modulation of miR-155 and miR-125b Levels following Lipopolysaccharide/TNF-Stimulation and Their possible roles in regulating the response to endotoxin shock. *J. Immunol.*, **15**, 5082–5089.
37. Pogue, A.I., Cui, J.G., Li, Y.Y., Zhao, Y., Culicchia, F. and Lukiw, W.J. (2010) Micro RNA-125b (miRNA-125b) function in astrogliosis and glial cell proliferation. *Neurosci. Lett.*, **476**, 18–122.
38. Hebert, S.S. and De Strooper, B. (2009) Alterations of the microRNA network cause neurodegenerative disease. *Trends Neurosci.*, **32**, 199–206.
39. Delay, C. and Hebert, S.S. (2011) MicroRNAs and Alzheimer's disease mouse models: current insights and future research avenues. *Int. J. Alzheimers Dis.*, **2011**, 894938.
40. Tarassishin, L., Loudig, O., Bauman, A., Shafit-Zagardo, B., Suh, H.S. and Lee, S.C. (2011) Interferon regulatory factor 3 inhibits astrocyte inflammatory gene expression through suppression of the proinflammatory miR-155 and miR-155*. *Glia*, **59**, 1911–1922.
41. Ponomarev, E.D., Veremeyko, T. and Weiner, H.L. (2013) MicroRNAs are universal regulators of differentiation, activation, and polarization of microglia and macrophages in normal and diseased CNS. *Glia*, **61**, 91–103.
42. Yao, R., Ma, Y.L., Liang, W., Li, H.H., Ma, Z.J., Yu, X. and Liao, Y.H. (2012) MicroRNA-155 modulates Treg and Th17 cells differentiation and Th17 cell function by targeting SOCS1. *PLoS One*, **7**, e46082.
43. Yoshimura, A., Naka, T. and Kubo, M. (2007) SOCS proteins, cytokine signalling and immune regulation. *Nat. Rev. Immunol.*, **7**, 454–465.
44. Baker, B.J., Akhtar, L.N. and Benveniste, E.N. (2009) SOCS1 and SOCS3 in the control of CNS immunity. *Trends Immunol.*, **30**, 392–400.
45. Ma, X., Becker Buscaglia, L.E., Barker, J.R. and Li, Y. (2011) MicroRNAs in NF-kappaB signaling. *J. Mol. Cell Biol.*, **3**, 159–166.
46. Jones, L., Holmans, P.A., Hamshere, M.L., Harold, D., Moskvina, V., Ivanov, D., Pocklington, A., Abraham, R., Hollingworth, P., Sims, R. *et al.* (2010) Genetic evidence implicates the immune system and cholesterol metabolism in the aetiology of Alzheimer's disease. *PLoS One*, **5**, e13950.
47. Holmans, P., Moskvina, V., Jones, L., Sharma, M., International Parkinson's Disease Genomics Consortium, Vedernikov, A., Buchel, F., Saad, M., Bras, J.M., Bettella, F. *et al.* (2013) A pathway-based analysis provides additional support for an immune-related genetic susceptibility to Parkinson's disease. *Hum. Mol. Genet.*, **22**, 1039–1049.
48. Guerreiro, R., Wojtas, A., Bras, J., Carrasquillo, M., Rogaeva, E., Majounie, E., Cruchaga, C., Sassi, C., Kauwe, J.S., Younkin, S. *et al.* (2013) TREM2 variants in Alzheimer's disease. *N. Engl. J. Med.*, **368**, 117–127.
49. Guerreiro, R.J., Santana, I., Bras, J.M., Santiago, B., Paiva, A. and Oliveira, C. (2007) Peripheral inflammatory cytokines as biomarkers in Alzheimer's disease and mild cognitive impairment. *Neurodegener. Dis.*, **4**, 406–412.
50. Albert, M.S., DeKosky, S.T., Dickson, D., Dubois, B., Feldman, H.H., Fox, N.C., Gamst, A., Holtzman, D.M., Jagust, W.J., Petersen, R.C. *et al.* (2011) The diagnosis of mild cognitive impairment due to Alzheimer's disease: recommendations from the National Institute on Aging-Alzheimer's Association workgroups on diagnostic guidelines for Alzheimer's disease. *Alzheimers Dement*, **7**, 270–279.
51. Wyss-Coray, T. (2006) Inflammation in Alzheimer disease: driving force, bystander or beneficial response? *Nat. Med.*, **12**, 1005–1015.
52. Rivest, S. (2009) Regulation of innate immune responses in the brain. *Nat. Rev. Immunol.*, **9**, 429–439.
53. Krabbe, G., Halle, A., Matyash, V., Rinnenthal, J.L., Eom, G.D., Bernhardt, U., Miller, K.R., Prokop, S., Kettenmann, H. and Heppner, F.L. (2013) Functional impairment of microglia coincides with Beta-amyloid deposition in mice with Alzheimer-like pathology. *PLoS One*, **8**, e60921.
54. Varnum, M.M. and Ikezu, T. (2012) The classification of microglial activation phenotypes on neurodegeneration and regeneration in Alzheimer's disease brain. *Arch. Immunol. Ther. Exp. (Warsz.)*, **60**, 251–266.
55. Callizot, N., Combes, M., Steinschneider, R. and Poindron, P. (2013) Operational dissection of beta-amyloid cytopathic effects on cultured neurons. *J. Neurosci. Res.*, **91**, 706–716.
56. Oddo, S., Caccamo, A., Shepherd, J.D., Murphy, M.P., Golde, T.E., Kayed, R., Metherate, R., Mattson, M.P., Akbari, Y. and LaFerla, F.M. (2003) Triple-transgenic model of Alzheimer's disease with plaques and tangles: intracellular Abeta and synaptic dysfunction. *Neuron*, **39**, 409–421.
57. Rebeck, G.W., Hoe, H.S. and Moussa, C.E. (2010) Beta-amyloid1–42 gene transfer model exhibits intraneuronal amyloid, gliosis, tau phosphorylation, and neuronal loss. *J. Biol. Chem.*, **285**, 7440–7446.
58. Takaoka, A. and Yanai, H. (2006) Interferon signalling network in innate defence. *Cell Microbiol.*, **8**, 907–922.
59. Khandelwal, P.J., Herman, A.M. and Moussa, C.E. (2011) Inflammation in the early stages of neurodegenerative pathology. *J. Neuroimmunol.*, **238**, 1–11.
60. Zaheer, S., Thangavel, R., Wu, Y., Khan, M.M., Kempuraj, D. and Zaheer, A. (2013) Enhanced expression of glia maturation factor correlates with glial activation in the brain of triple transgenic Alzheimer's disease mice. *Neurochem. Res.*, **38**, 218–225.
61. Qin, H., Wilson, C.A., Lee, S.J. and Benveniste, E.N. (2006) IFN-beta-induced SOCS-1 negatively regulates CD40 gene expression in macrophages and microglia. *FASEB J.*, **20**, 985–987.
62. Costa, P.M., Cardoso, A.L., Mendonca, L.S., Serani, A., Custodia, C., Conceicao, M., Simoes, S., Moreira, J.N., Pereira de Almeida, L. and Pedroso de Lima, M.C. (2013) Tumor-targeted chlorotoxin-coupled nanoparticles for nucleic acid delivery to glioblastoma cells: A promising system for glioblastoma treatment. *Mol. Ther. Nucleic Acids*, **2**, e100.
63. Worm, J., Stenvang, J., Petri, A., Frederiksen, K.S., Obad, S., Elmen, J., Hedtjarn, M., Straarup, E.M., Hansen, J.B. and Kauppinen, S. (2009) Silencing of microRNA-155 in mice during acute inflammatory response leads to derepression of c/ebp Beta and down-regulation of G-CSF. *Nucleic Acids Res.*, **37**, 5784–5792.
64. Gatto, G., Rossi, A., Rossi, D., Kroening, S., Bonatti, S. and Mallardo, M. (2008) Epstein–Barr virus latent membrane protein 1 trans-activates miR-155 transcription through the NF-kappaB pathway. *Nucleic Acids Res.*, **36**, 6608–6619.
65. Guo, Q., Fu, W., Sopher, B.L., Miller, M.W., Ware, C.B., Martin, G.M. and Mattson, M.P. (1999) Increased vulnerability of hippocampal neurons to excitotoxic necrosis in presenilin-1 mutant knock-in mice. *Nat. Med.*, **5**, 101–106.
66. Simoes, A.T., Goncalves, N., Koeppen, A., Deglon, N., Kugler, S., Duarte, C.B. and Pereira de Almeida, L. (2012) Calpastatin-mediated inhibition of calpains in the mouse brain prevents mutant ataxin 3 proteolysis, nuclear localization and aggregation, relieving Machado–Joseph disease. *Brain*, **135**, 2428–2439.
67. Resende, R., Ferreiro, E., Pereira, C. and Resende de Oliveira, C. (2008) Neurotoxic effect of oligomeric and fibrillar species of amyloid-beta peptide 1–42: involvement of endoplasmic reticulum calcium release in oligomer-induced cell death. *Neuroscience*, **155**, 725–737.
68. Lu, J. and Tsourkas, A. (2009) Imaging individual microRNAs in single mammalian cells in situ. *Nucleic Acids Res.*, **37**, e100.